N.B. Ladygina

REACTION MECHANISMS IN DEUTERON-PROTON ELASTIC SCATTERING AT INTERMEDIATE ENERGIES

- **The theoretical model is suggested for description of both differential cross section and polarization observables in the deuteron energy range between 500 and 2000 MeV.**
- $dp \to dp$ **reaction is considered in the full angular range.**
- **The calculation results are presented in comparison with the data.**

$dp \to dp$

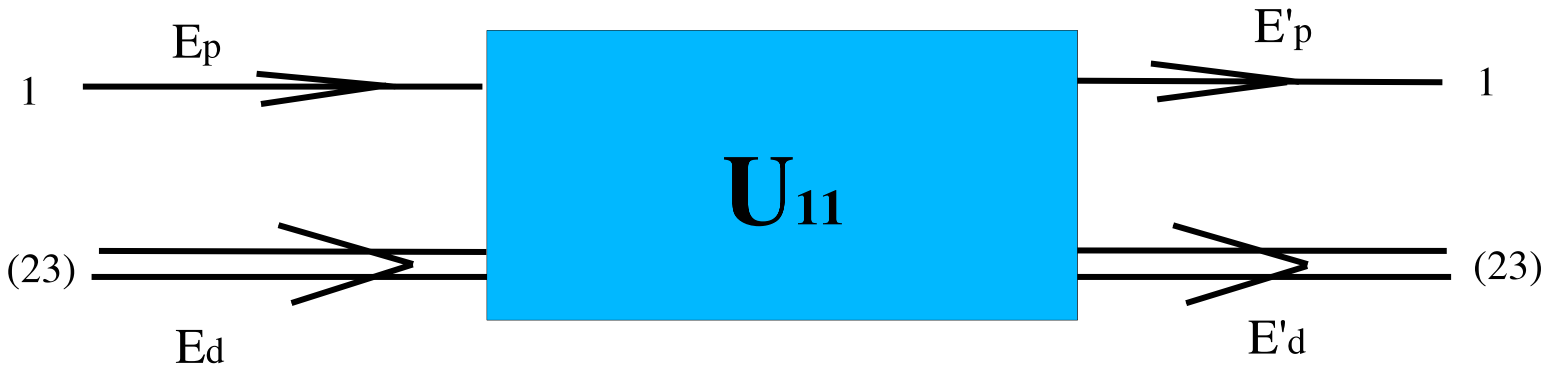

The matrix element of the transition operator U_{11} defines reaction amplitude

$$U_{dp\to dp} = \delta(E_d + E_p - E'_d - E'_p)\mathcal{J} =< 1(23)|[1 - P_{12} - P_{13}]U_{11}|1(23) >$$

Alt-Grassberger-Sandhas equations for rearrangement operators:
Nucl.Phys. B2, 167 (1967)
E.Schmid, H.Ziegelmann The Quantum Mechanical Three-Body Problem

$$
\begin{aligned}
U_{11} &= t_{13} g_0 U_{21} + t_{12} g_0 U_{31} \\
U_{21} &= g_0^{-1} + t_{23} g_0 U_{11} + t_{12} g_0 U_{31} \\
U_{31} &= g_0^{-1} + t_{23} g_0 U_{11} + t_{13} g_0 U_{21}
\end{aligned}
$$

$t_1 = t(2,3)$**, etc., is the** t**-matrix of the two-particle interaction**
g_0 **is the free three-particle propagator**
Iterating AGS-equations up to second order terms over t **one obtains**

$$
U_{11} = -2P_{12} g_0^{-1} + 2t_{12}^{sym} + 2t_{12}^{sym} g_0 t_{13}^{sym}
$$

$t_{ij}^{sym} = [1 - P_{ij}] t_{ij}$**– antisymmetrized t-matrix**

Diagrams

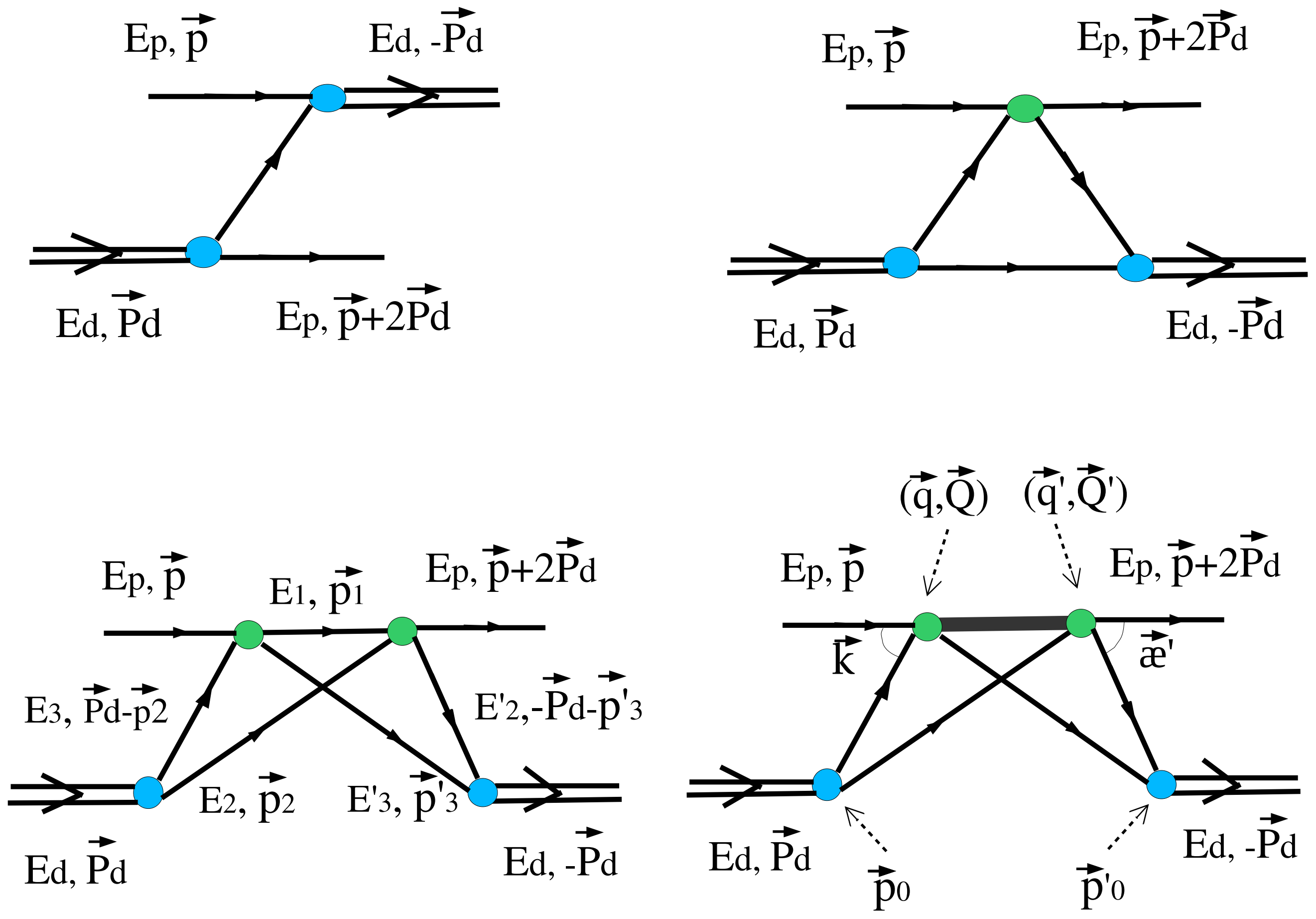

Ep, p
Ed, -Pd
Ed, Pd
Ep, p+2Pd
Ep, p
Ep, p+2Pd
Ed, Pd
Ed, -Pd
Ep, p
E1, p1
Ep, p+2Pd
E3, Pd-p2
E'2,-Pd-p'3
E2, p2
E'3, p'3
Ed, Pd
Ed, -Pd
(q,Q)
(q',Q')
Ep, p
Ep, p+2Pd
k
æ'
Ed, Pd
Ed, -Pd
p0
p'0

Deuteron rest frame

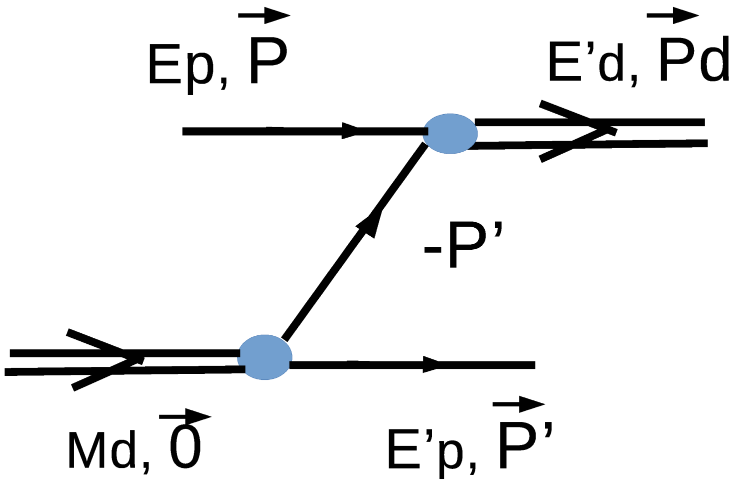

$$\vec{p}_0 \approx \vec{P}'$$

$$\vec{p}_0' \approx \frac{1}{2}(\vec{P} + \vec{P}')$$

$$\mathcal{J}_{ONE} \sim_{1(23)}< \vec{p}' m'; \vec{P}_d \mathcal{M}'_d | \Omega_d^\dagger(23) P_{12} \Omega_d(23) | \vec{0} \mathcal{M}_d; \vec{p} m >_{1(23)}$$

Breit system

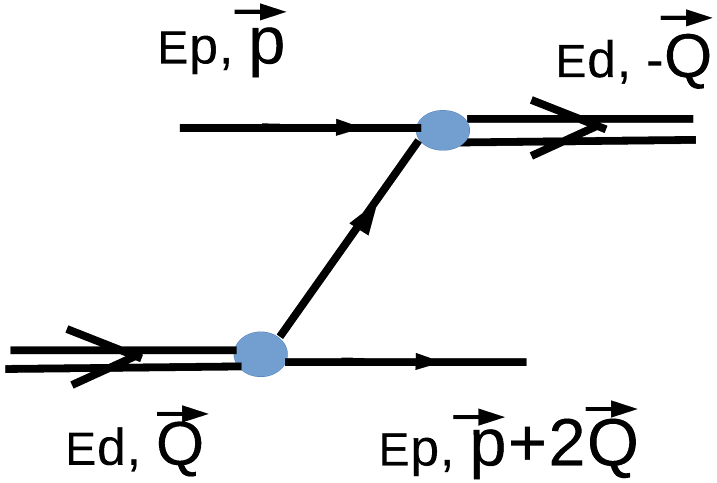

$$E_d = E_d' = \sqrt{M_d^2 + \vec{Q}^2}$$
$$E_p = E_p' = \sqrt{m^2 + \vec{p}^2}$$
$$(\vec{p}\vec{Q}) = -\vec{Q}^2$$

$$|\vec{p}_0| = |\vec{p}_0{}'| \approx \sqrt{\vec{p}^2_{Breit} - \frac{3}{4}\vec{Q}^2_{Breit}}$$

$$\mathcal{J}_{ONE} \sim_{1(23)}< \vec{p}' m'; -\vec{Q}\mathcal{M}_d'|\Omega_d^\dagger(23)P_{12}\Omega_d(23)|\vec{Q}\mathcal{M}_d; \vec{p}m >_{1(23)}$$

Lorenz transformation

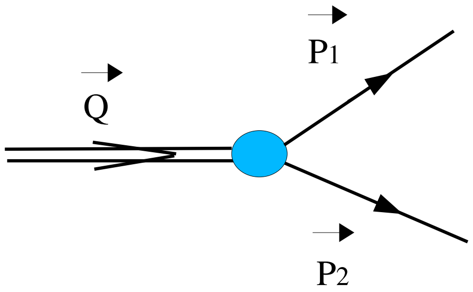

$$L(\vec{u})p_1 = (E^*, \vec{p})$$
$$L(\vec{u})p_2 = (E^*, -\vec{p})$$

with velocity

$$\vec{u} = \frac{\vec{p}_1 + \vec{p}_2}{E_1 + E_2}$$

The c.m. energy of one of the nucleons E^* is related with Mandelstam variable s by

$$E^* = \sqrt{s}/2 \quad .$$

Let's introduce new variables $\vec{Q}$ and $\vec{k}$ which can be expressed through $\vec{p}_1$ and $\vec{p}_2$

$$\vec{P} = \vec{p}_1 + \vec{p}_2$$
$$\vec{p} = \frac{(E_2 + E^*)\vec{p}_1 - (E_1 + E^*)\vec{p}_2}{E_1 + E_2 + 2E^*} \quad .$$

Deuteron wave function

The deuteron wave function in the rest has the standard form

$$< m_p m_n, \vec{p}|\Omega_d|\vec{0}, \mathcal{M}_d >=$$
$$\frac{1}{\sqrt{4\pi}} < m_p m_n, \vec{p}| \left\{ u(p) + \frac{w(p)}{\sqrt{8}} [3(\vec{\sigma}_1 \hat{p})(\vec{\sigma}_2 \hat{p}) - (\vec{\sigma}_1 \vec{\sigma}_2)] \right\} |\vec{0} \mathcal{M}_d >$$

$u(p)$ **and** $w(p)$ **-** $S-$ **and** $D-$ **components of the deuteron.**
Then the deuteron wave function in the moving frame is

$$< \vec{p}_1 \ \vec{p}_2, m_1 m_2 |\Omega_d| \vec{Q}, \mathcal{M}_d > \quad \sim \quad < \vec{p}, m_1' m_2' | W^{\dagger}_{1/2}(\vec{p}_1, \vec{u}) W^{\dagger}_{1/2}(\vec{p}_2, \vec{u}) \Omega_d |\vec{0}, \mathcal{M}_d >$$

where $W_{1/2}$ **is Wigner rotation operator**

$$W_{1/2}(\vec{p}_i, \vec{u}) = exp\{-i\omega_i(\vec{n}_i\vec{\sigma}_i)/2\} = cos(\omega_i/2)[1 - i(\vec{n}_i\vec{\sigma}_i)tg(\omega_i/2)]$$
$$\vec{n}_i = \frac{\vec{p}_i \times \vec{u}}{|\vec{p}_i \times \vec{u}|}$$

Deuteron wave function in the moving frame

$$
\begin{aligned}
& < \vec{p}_1\ \vec{p}_2, m_1 m_2 | \Omega_d | \vec{Q}, \mathcal{M}_d >= \\
& < \vec{k}(\vec{p}_1, \vec{p}_2), m_1 m_2 | g_1(\vec{k}, \vec{Q}) + g_2(\vec{k}, \vec{Q})(\vec{\sigma}_1 \vec{n})(\vec{\sigma}_2 \vec{n}) + \\
+ \quad & g_3(\vec{k}, \vec{Q})(\vec{\sigma}_1 \vec{\sigma}_2) + g_4(\vec{k}, \vec{Q})(\vec{\sigma}_1 \hat{k})(\vec{\sigma}_2 \hat{k}) + + g_5(\vec{k}, \vec{Q})[(\vec{\sigma}_1 + \vec{\sigma}_2)\vec{n}] + \\
+ \quad & g_6(\vec{k}, \vec{Q})[(\vec{\sigma}_1 \hat{k})(\vec{\sigma}_2 \vec{n} \times \hat{k}) + (\vec{\sigma}_1 \vec{n} \times \hat{k})(\vec{\sigma}_2 \hat{k})] | \vec{Q}, \mathcal{M}_d >
\end{aligned}
$$

g_i **are combinations of the** $S-$ **and** $D-$ **components of the deuteron wave function (**u **and** w**)**

Single Scattering contribution

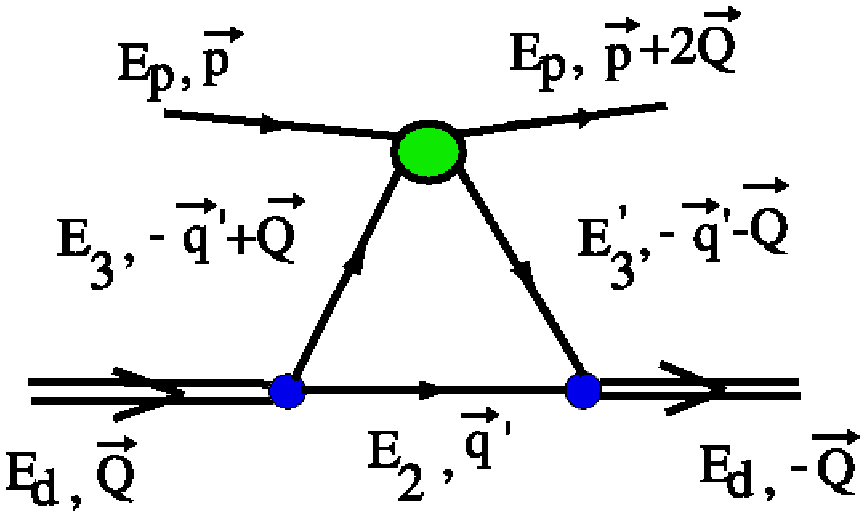

$$\mathcal{J}_{SS} =_{1(23)}< \vec{p}' m'; -\vec{Q}\mathcal{M}'_d|\Omega^{\dagger}_d(23)|[1 - P_{12}]|t_{NN}\Omega_d(23)|\vec{Q}\mathcal{M}_d; \vec{p}m >_{1(23)}$$

Nucleon-Nucleon t-matrix

W.G.Love, M.A.Franey, Phys.Rev.C24, 1073 (1981)
N.B.Ladygina,nucl-th/0805.3021

$$
\begin{aligned}
< \kappa' m_1' m_2' | t | \kappa m_1 m_2 > \quad = \quad & < \vec{\kappa}' m_1' m_2' | A + B(\vec{\sigma}_1 \hat{N}^*)(\vec{\sigma}_2 \hat{N}^*) + C(\vec{\sigma}_1 + \vec{\sigma}_2) \cdot \hat{N}^* + \\
& D(\vec{\sigma}_1 \hat{q}^*)(\vec{\sigma}_2 \hat{q}^*) + F(\vec{\sigma}_1 \hat{Q}^*)(\vec{\sigma}_2 \hat{Q}^*) | \vec{\kappa} m_1 m_2 >
\end{aligned}
$$

where the orthonormal basis is combinations of the nucleons relative momenta in the initial $\vec{\kappa}$ and final $\vec{\kappa}'$ states

$$
\hat{q}^* = \frac{\vec{\kappa} - \vec{\kappa}'}{|\vec{\kappa} - \vec{\kappa}'|} \quad , \quad \hat{Q}^* = \frac{\vec{\kappa} + \vec{\kappa}'}{|\vec{\kappa} + \vec{\kappa}'|} \quad , \quad \hat{N}^* = \frac{\vec{\kappa} \times \vec{\kappa}'}{|\vec{\kappa} \times \vec{\kappa}'|}
$$

The amplitudes A, B, C, D, F are the functions of the center-of-mass energy and scattering angle. The radial parts of these amplitudes are taken as a sum of Yukawa terms.

Nucleon-Nucleon t-matrix

NN t-matrix in orbitrary frame is related to t-matrix in the center-mass as follows:

$$< \vec{p}_1' \vec{p}_2'; m_1' m_2' | t | \vec{p}_1 \vec{p}_2; m_1 m_2 > \sim$$
$$< \kappa' m_1' m_2' | W^{\dagger}_{1/2}(\vec{p}_1') W^{\dagger}_{1/2}(\vec{p}_2') \ t_{cm} \ W_{1/2}(\vec{p}_1) W_{1/2}(\vec{p}_2) | \kappa m_1 m_2 >$$

Double scattering contribution

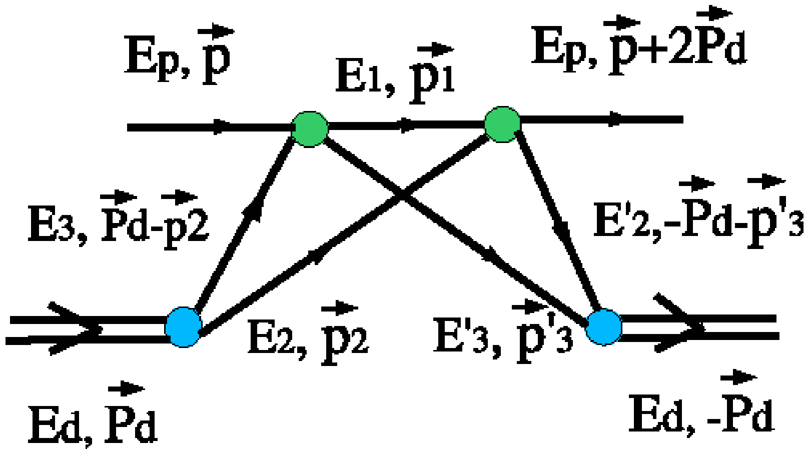

$$
\begin{aligned}
\mathcal{J}_\Delta = \quad & < 1(23)|[1 - P_{12}]|t_{NN}|N(1)N(2) > |N(3) > g_0 \\
& < N(2)| < N(1)N(3)|t_{NN}[1 - P_{13}]|(23)1 >
\end{aligned}
$$

g_0 **is a free three-particle propagator:**

$$
\begin{aligned}
g_0 &= \frac{1}{E_d + E_p - E_1 - E_2 - E_3' + i\varepsilon} = \\
&= \mathcal{P}\frac{1}{E_d + E_p - E_1 - E_2 - E_3'} - i\pi\delta(E_d + E_p - E1 - E_2 - E_3')
\end{aligned}
$$

Δ-contribution

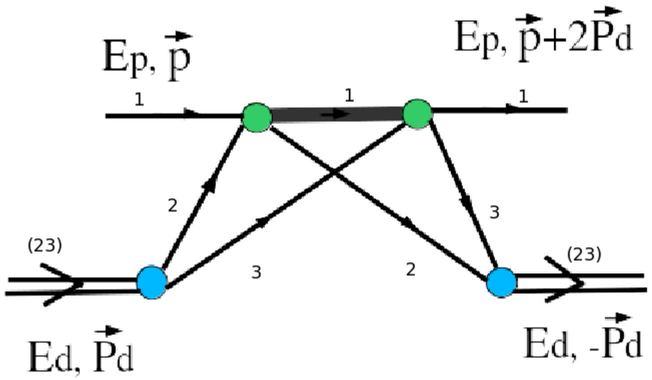

$$\mu^2 = E_\Delta^2 - \vec{p}_\Delta^{\,2}$$

Δ-contribution is defined by two $N\Delta$ matrices

$$\begin{aligned}\mathcal{J}_\Delta = \quad & < 1(23)|[1-P_{12}]|t_{N\Delta}|\Delta(1)N(2) > |N(3) > g_0 \\ & < N(2)| < \Delta(1)N(3)|t_{\Delta N}[1-P_{13}]|(23)1 >\end{aligned}$$

g_0–a free three-particle propagator:

$$g_0 = \frac{1}{E_d + E_p - E_2' - E_3 - E(m_\Delta) + i\Gamma(E_\Delta)/2}$$

the distribution function of Δ-energy:

$$\rho(\mu) = \frac{1}{2\pi}\frac{\Gamma(\mu)}{(E_\Delta(\mu) - E_\Delta(m_\Delta))^2 + \Gamma^2(\mu)/4},$$

and wave functions of the initial and final deuterons.

Δ-isobar definition

The potential for the $NN \to N\Delta$ transition is based on the $\pi-$ and $\rho-$ exchanges:

$$
\begin{aligned}
t_{N\Delta}^{(\pi)} &= -\frac{f_\pi f_\pi^*}{m_\pi^2} F_\pi^2(t) \frac{q^2}{m_\pi^2 - t} (\vec{\sigma} \cdot \hat{q})(\vec{S} \cdot \hat{q})(\vec{\tau} \cdot \vec{T}) \\
t_{N\Delta}^{(\rho)} &= -\frac{f_\rho f_\rho^*}{m_\rho^2} F_\rho^2(t) \frac{q^2}{m_\rho^2 - t} \{(\vec{\sigma}\vec{S}) - (\vec{\sigma} \cdot \hat{q})(\vec{S} \cdot \hat{q})\}(\vec{\tau} \cdot \vec{T})
\end{aligned}
$$

with coupling constants:

$$
\begin{aligned}
f_\pi &= 1.008 \qquad f_\pi^* = 2.156 \\
f_\rho &= 7.8 \qquad f_\rho^* = 1.85 f_\rho
\end{aligned}
$$

The hadronic form factor has a pole form:

$$
F_x(t) = (\Lambda_x^2 - m_x^2)/(\Lambda_x^2 - t)^n, \qquad
\begin{aligned}
n &= 1 \quad \mathit{for}\ \pi - \mathit{meson} \\
n &= 2 \quad \mathit{for}\ \rho - \mathit{meson}
\end{aligned}
$$

The reaction amplitude is defined through 12 terms:

$$\mathcal{J}_{dp\to dp} =< 1M_d'| < \frac{1}{2}m'|F_1 + F_2(\vec{S}\vec{y}) + F_3 Q_{xx} + F_4 Q_{yy} +$$
$$F_5(\vec{\sigma}\vec{x})(\vec{S}\vec{x}) + F_6(\vec{\sigma}\vec{x})Q_{xx} + F_7(\vec{\sigma}\vec{y}) + F_8(\vec{\sigma}\vec{y})(\vec{S}\vec{y}) + F_9(\vec{\sigma}\vec{y})Q_{xx} +$$
$$F_{10}(\vec{\sigma}\vec{y})Q_{yy} + F_{11}(\vec{\sigma}\vec{z})(\vec{S}\vec{z}) + F_{12}(\vec{\sigma}\vec{z})Q_{yz}|\frac{1}{2}m > |1M_d >$$

σ_i, S_i **are the spin operators for** $s = 1/2$ **(Pauli matrices) and** $S = 1$
Q_{ij} **is the quadrupole tenzor:**

$$Q_{ij} = \frac{1}{2}(S_i S_j + S_j S_i) - \frac{2}{3}\delta_{ij}$$

$$\sigma \sim Tr(\mathcal{J}\mathcal{J}^\dagger), \quad A_y = \frac{Tr(\mathcal{J}S_y\mathcal{J}^\dagger)}{Tr(\mathcal{J}\mathcal{J}^\dagger)}, \quad A_{yy} = \frac{Tr(\mathcal{J}Q_{yy}\mathcal{J}^\dagger)}{Tr(\mathcal{J}\mathcal{J}^\dagger)}$$

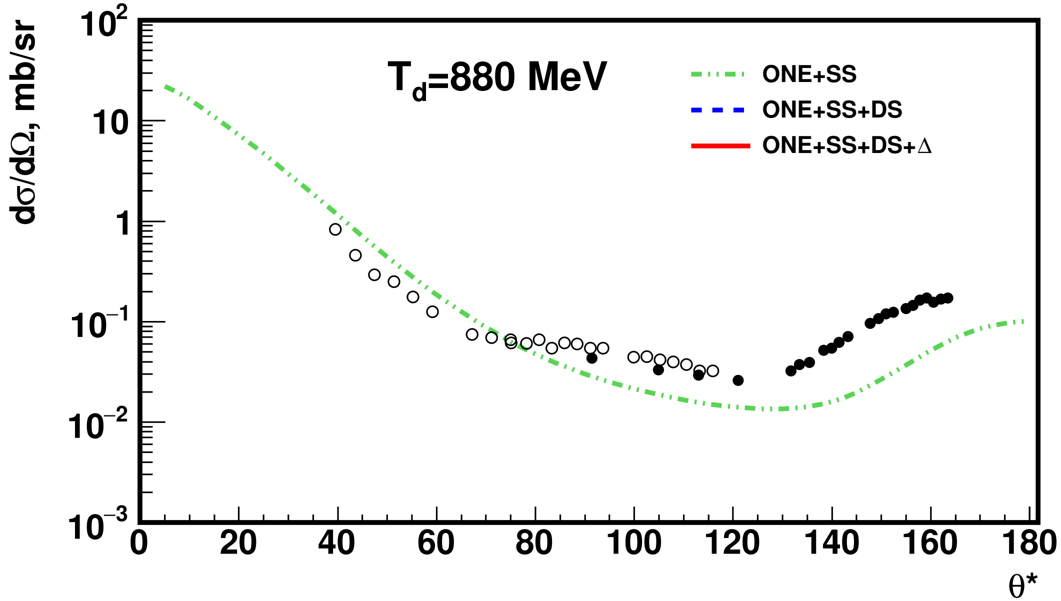

● - N.E.Booth et al., Phys.Rev.D4, p.1261 (1971), $T_d = 850 MeV$
○- J.C.Alder et al., Phys.Rev.C6, p.2010 (1972), $T_d = 940 MeV$

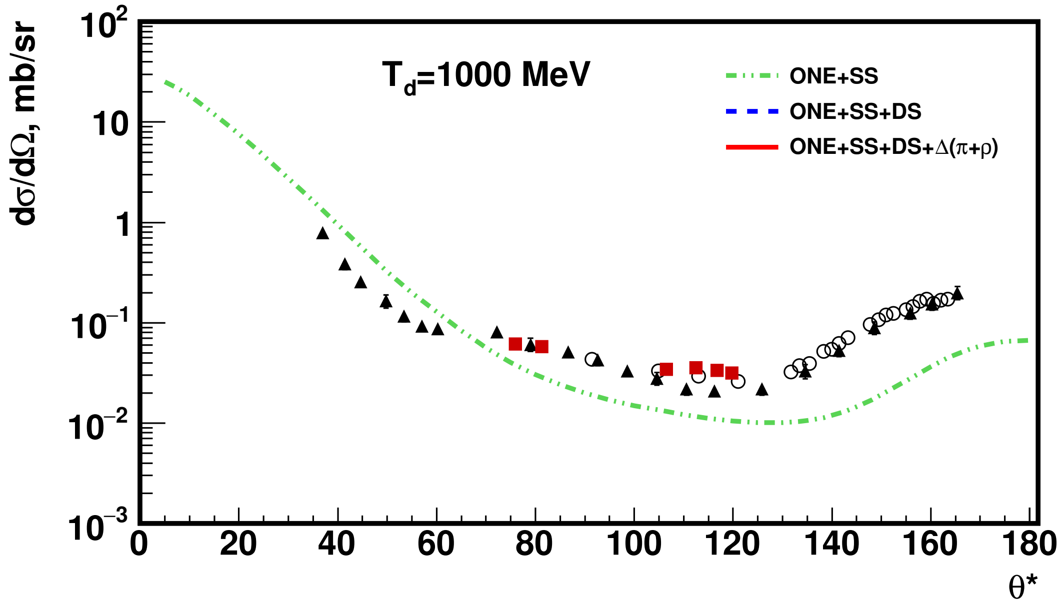

▲-J.S. Vincent et al., Phys. Rev. Lett. 24, 236 (1970), $T_d = 1160 MeV$
■ - A.A. Terekhin, et al., Eur. Phys. J. A55, 129(2019)

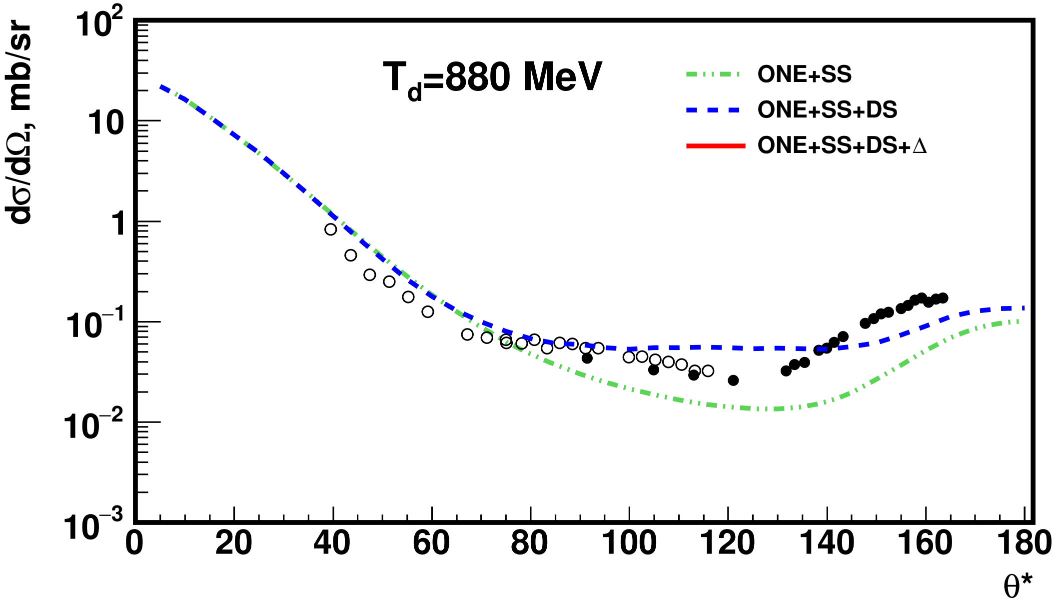

● - N.E.Booth et al., Phys.Rev.D4, p.1261 (1971), $T_d = 850 MeV$
○- J.C.Alder et al., Phys.Rev.C6, p.2010 (1972), $T_d = 940 MeV$

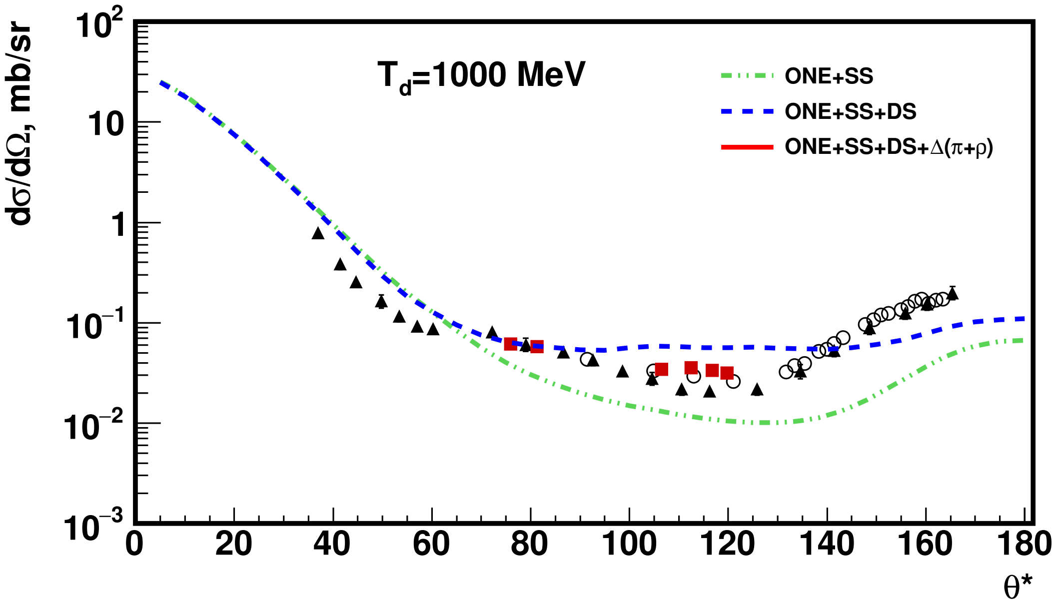

▲-J.S. Vincent et al., Phys. Rev. Lett. 24, 236 (1970), $T_d = 1160 MeV$
■ - A.A. Terekhin, et al., Eur. Phys. J. A55, 129(2019)

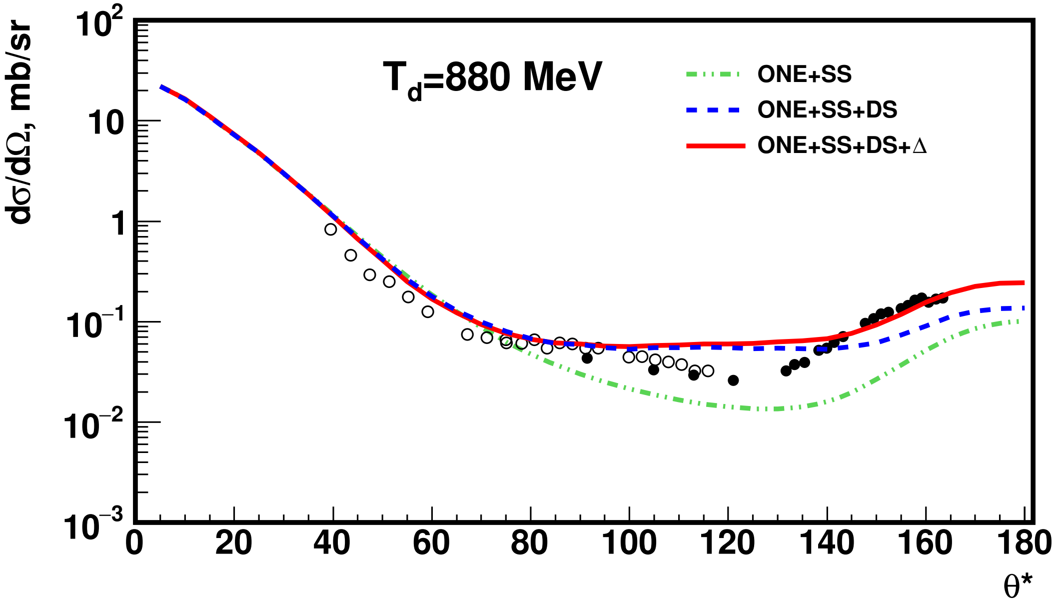

● - N.E.Booth et al., Phys.Rev.D4, p.1261 (1971), $T_d = 850 MeV$
○- J.C.Alder et al., Phys.Rev.C6, p.2010 (1972), $T_d = 940 MeV$

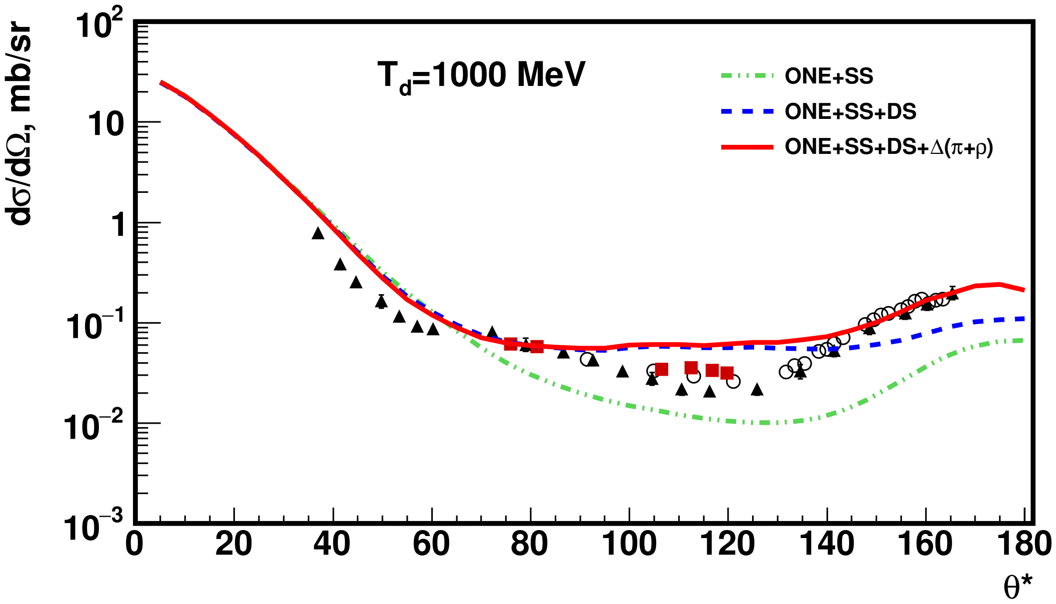

▲-J.S. Vincent et al., Phys. Rev. Lett. 24, 236 (1970), $T_d = 1160 MeV$
■ - A.A. Terekhin, et al., Eur. Phys. J. A55, 129(2019)

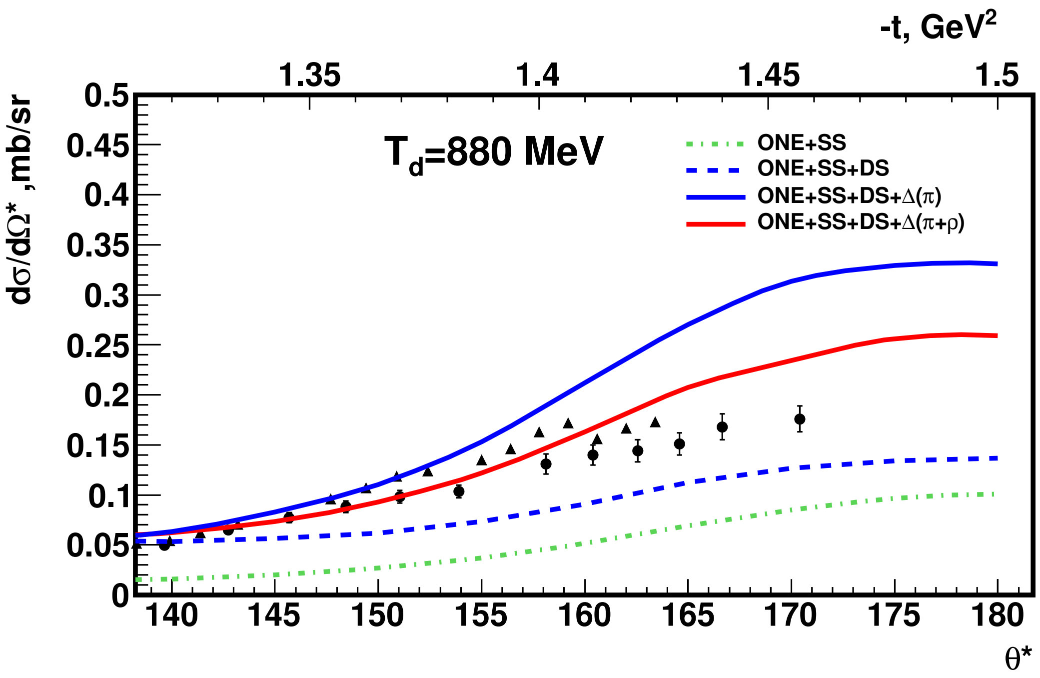

● - N.E.Booth et al., Phys.Rev.D4, p.1261 (1971), $T_d = 850 MeV$
▲- J.C.Alder et al., Phys.Rev.C6, p.2010 (1972), $T_d = 940 MeV$

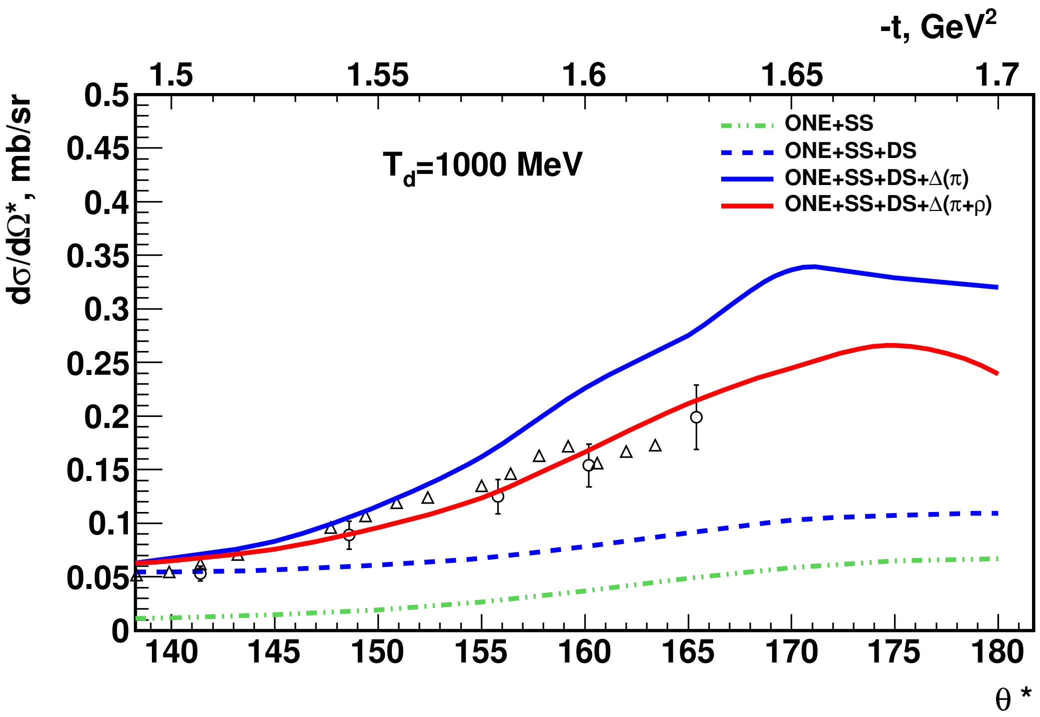

○-J.S.Vincent, Phys.Rev.Lett. 24, p.236 (1970), $T_d = 1169 MeV$
△- J.C.Alder et al., Phys.Rev.C6, p.2010 (1972), $T_d = 940 MeV$

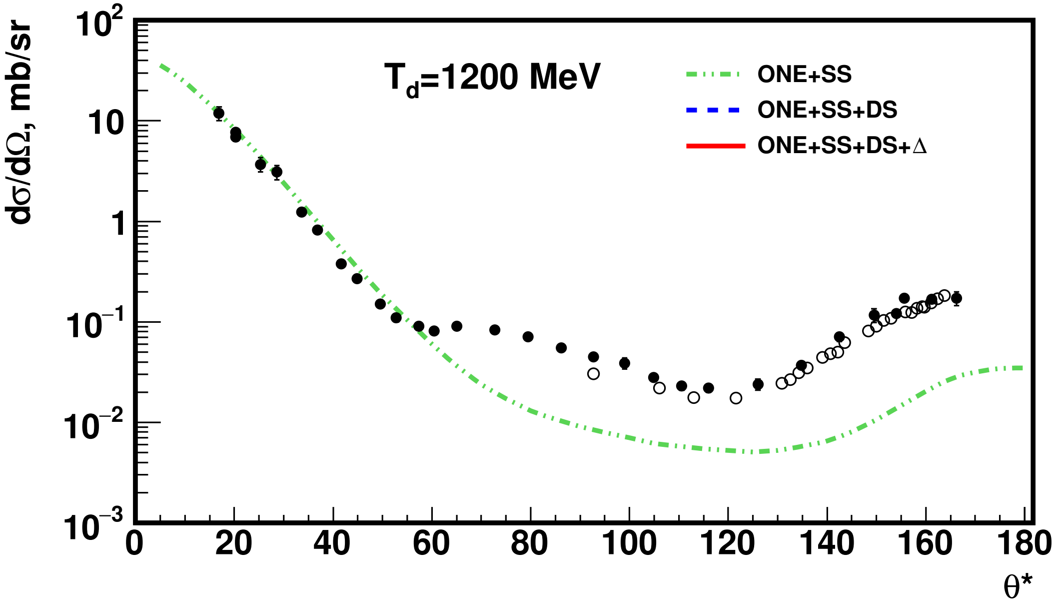

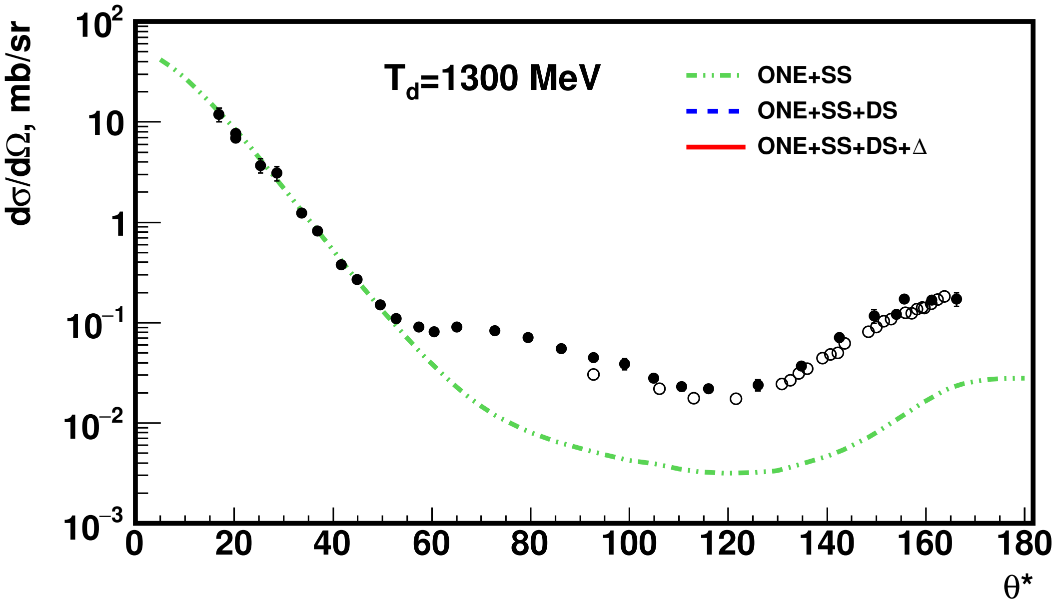

● - E.T.Boschitz et al.,Phys.Rev.C6, p.457 (1972)

○ - J.C.Alder et al.,Phys.Rev.C6, p.2010 (1972), $T_d = 1180 MeV$

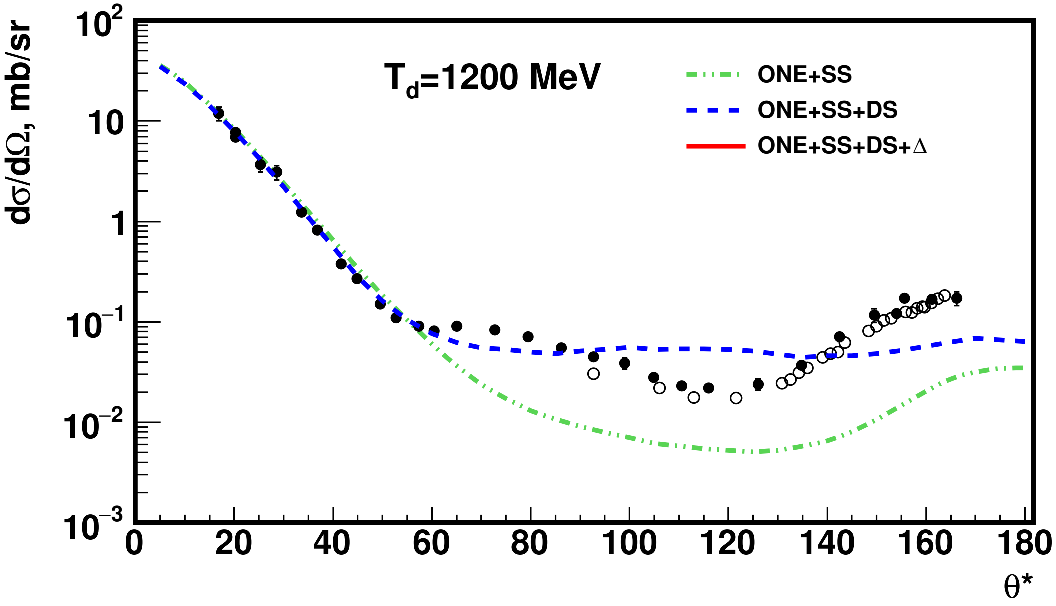

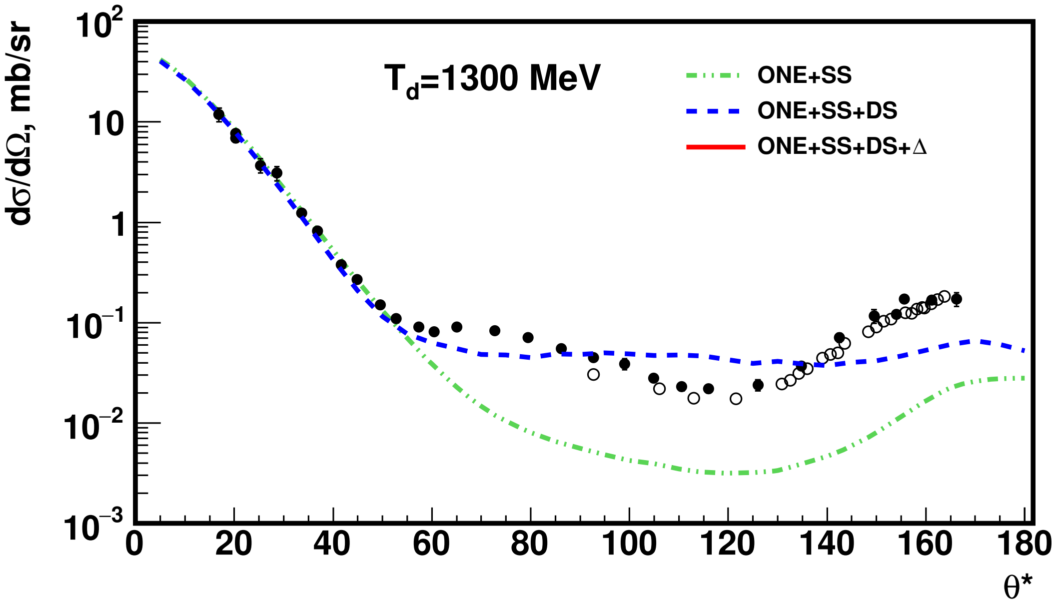

● - E.T.Boschitz et al.,Phys.Rev.C6, p.457 (1972)

○ - J.C.Alder et al.,Phys.Rev.C6, p.2010 (1972), $T_d = 1180 MeV$

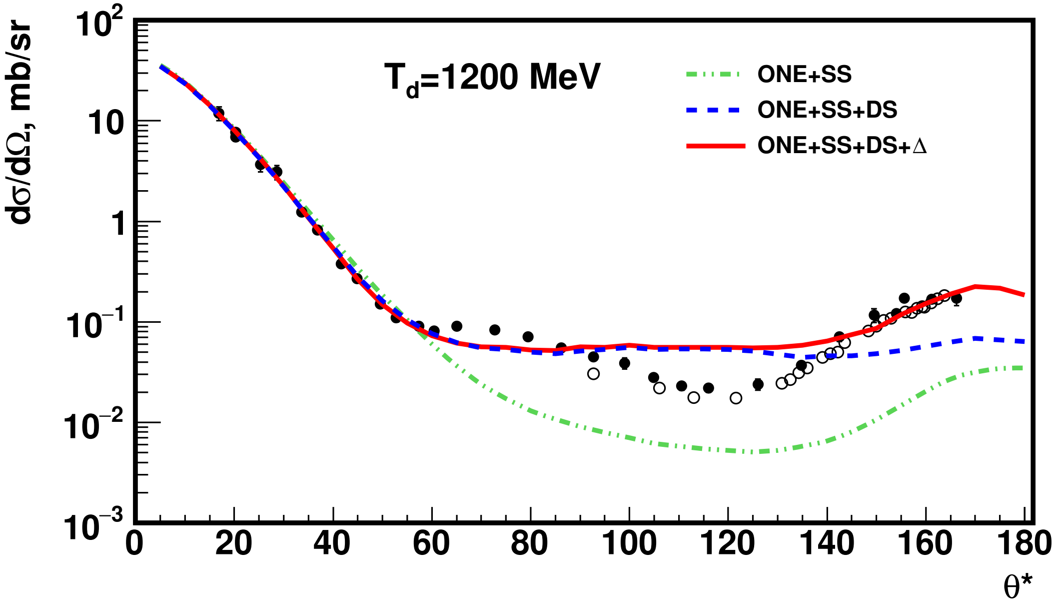

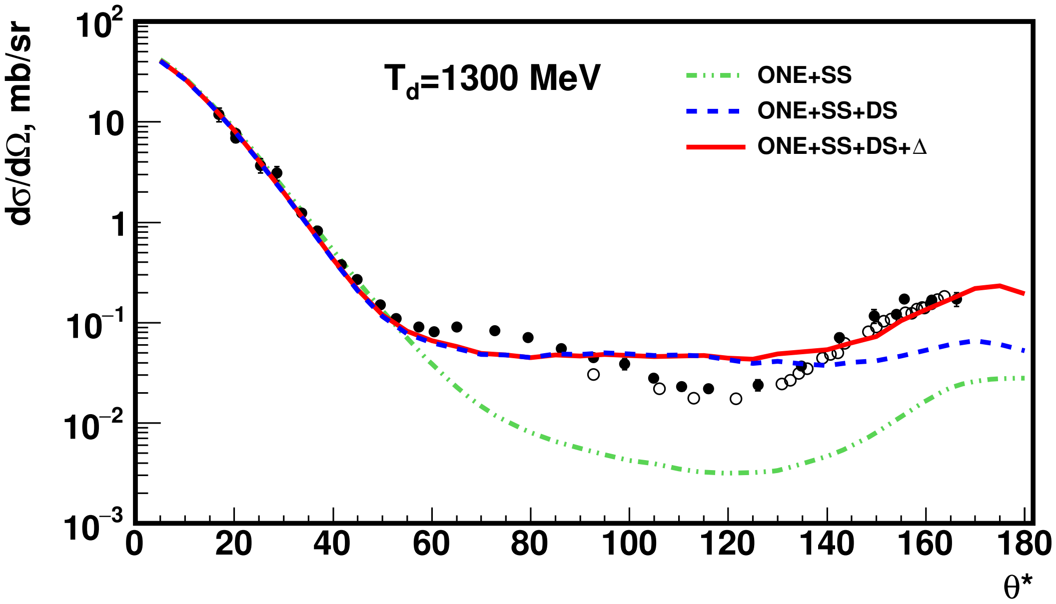

● - E.T.Boschitz et al.,Phys.Rev.C6, p.457 (1972)

○ - J.C.Alder et al.,Phys.Rev.C6, p.2010 (1972), $T_d = 1180 MeV$

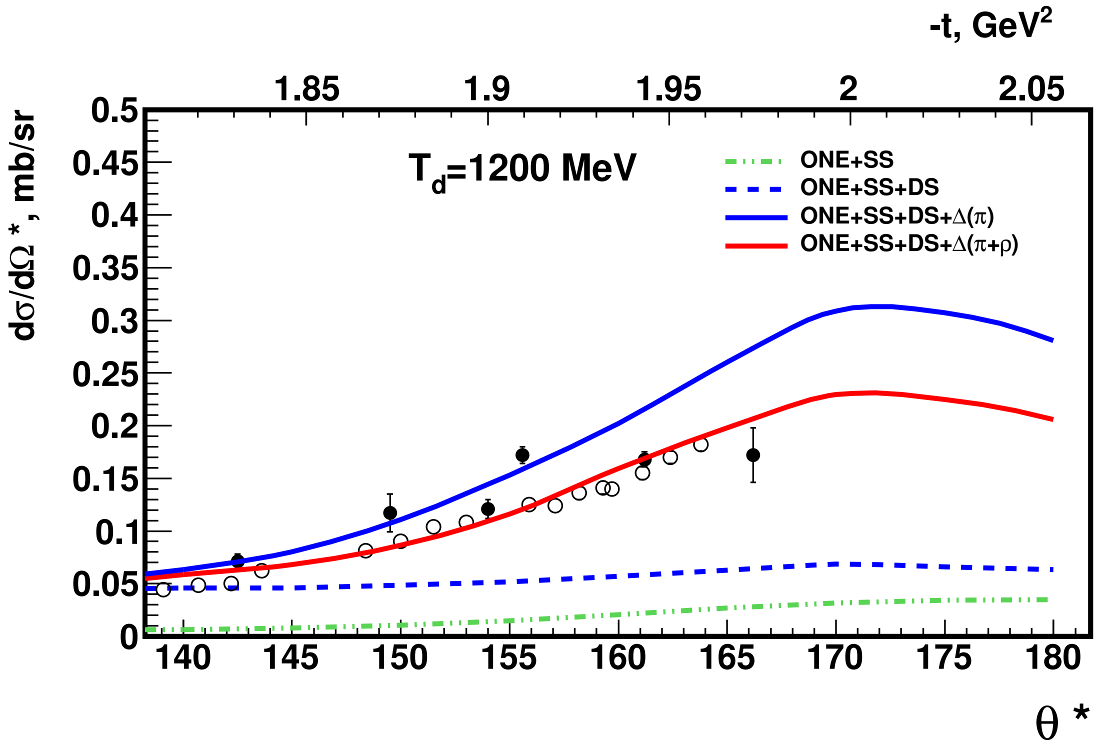

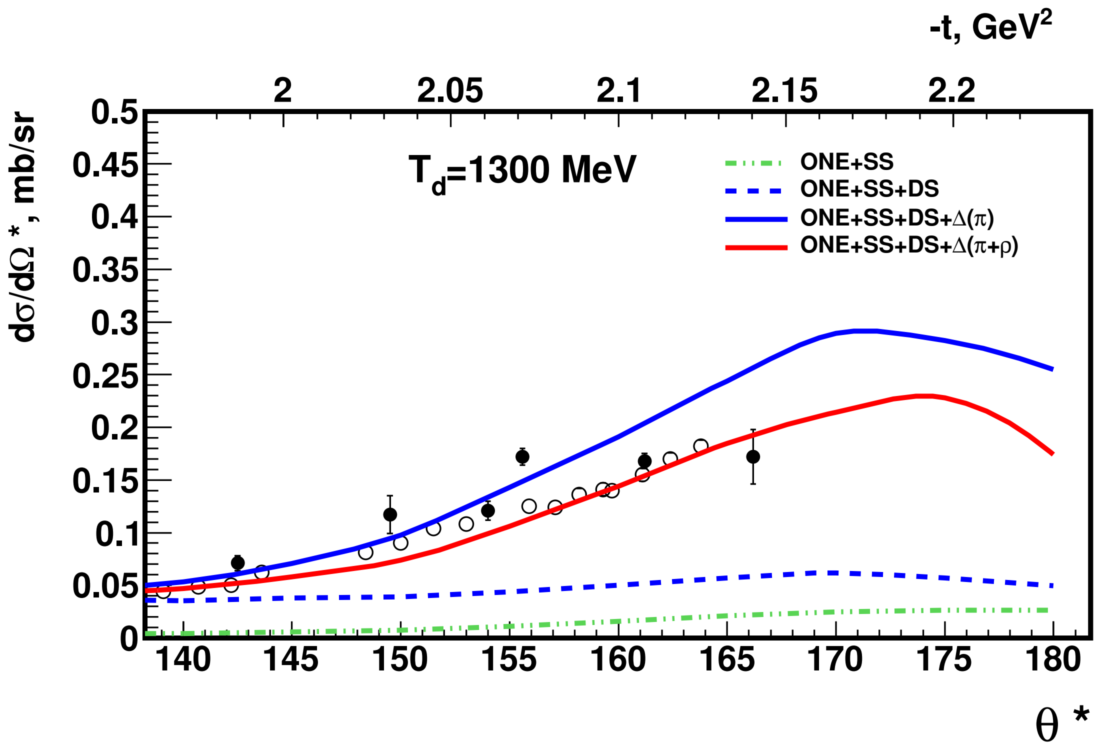

● - E.T.Boschitz et al.,Phys.Rev.C6, p.457 (1972)

○ - J.C.Alder et al.,Phys.Rev.C6, p.2010 (1972)

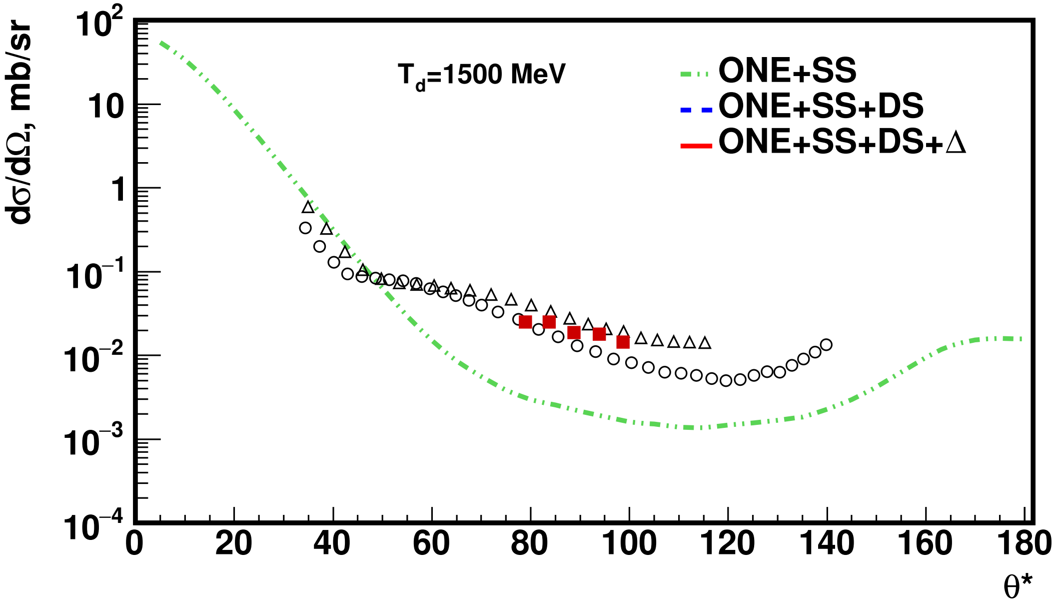

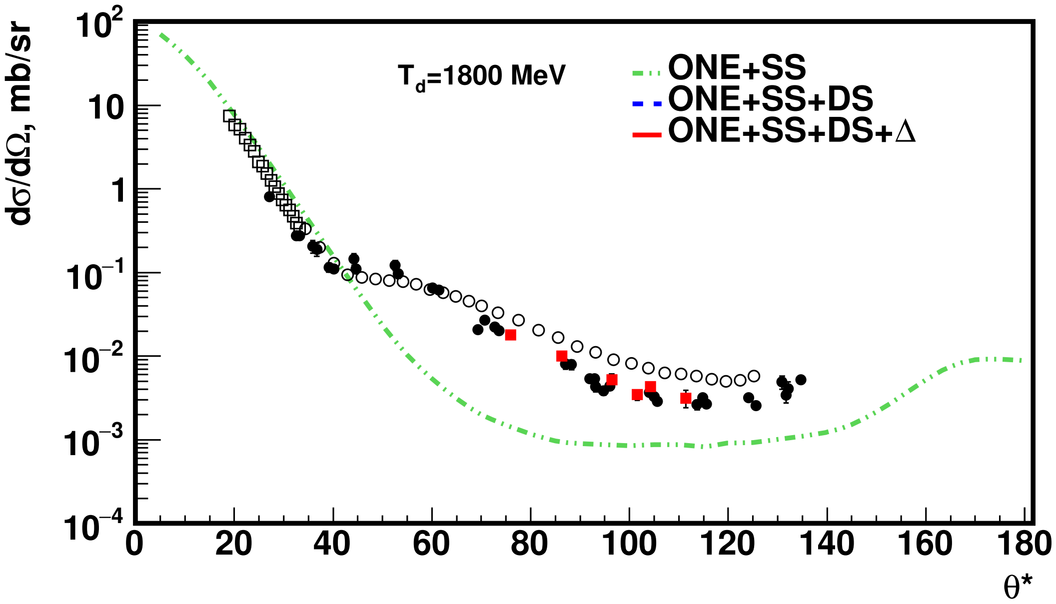

○ - E.Gülmez et al., Phys.Rev.C42, p.2067, 1991, $T_d = 1.585\,GeV$

△ - E.Gülmez et al., Phys.Rev.C42, p.2067, 1991, $T_d = 1.286\,GeV$

■ - A.A. Terekhin, et al., Eur. Phys. J. A55, 129(2019)

□ - C. Fritzsch et al., Phys.Lett.B 784, 277 (2018), $T_d = 1.8\,GeV$

● -Bennet et al., Phys. Rev. Lett. 19, p.387 (1967), $T_d = 2\,GeV$

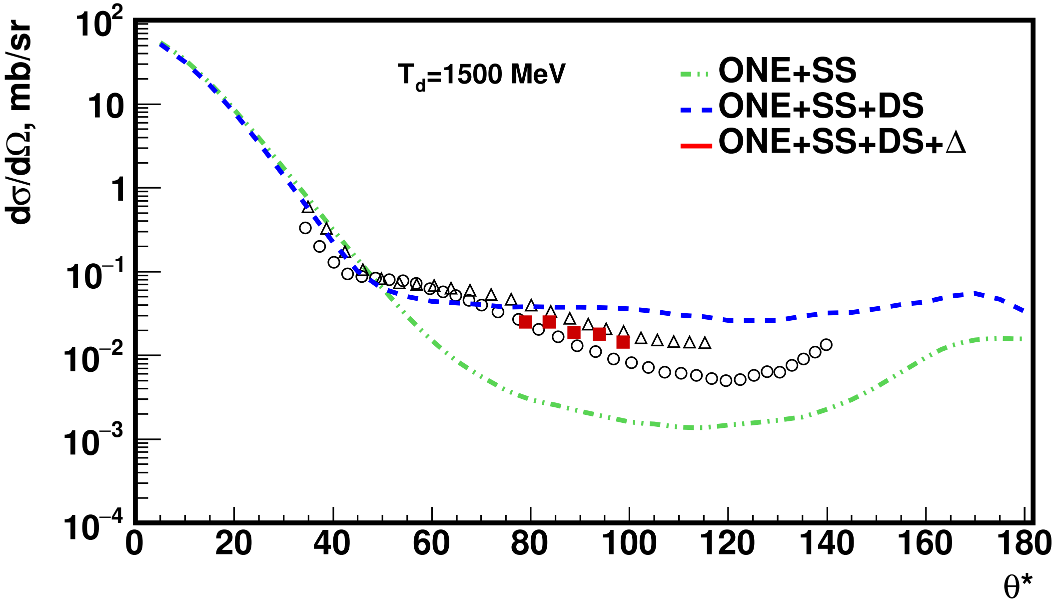

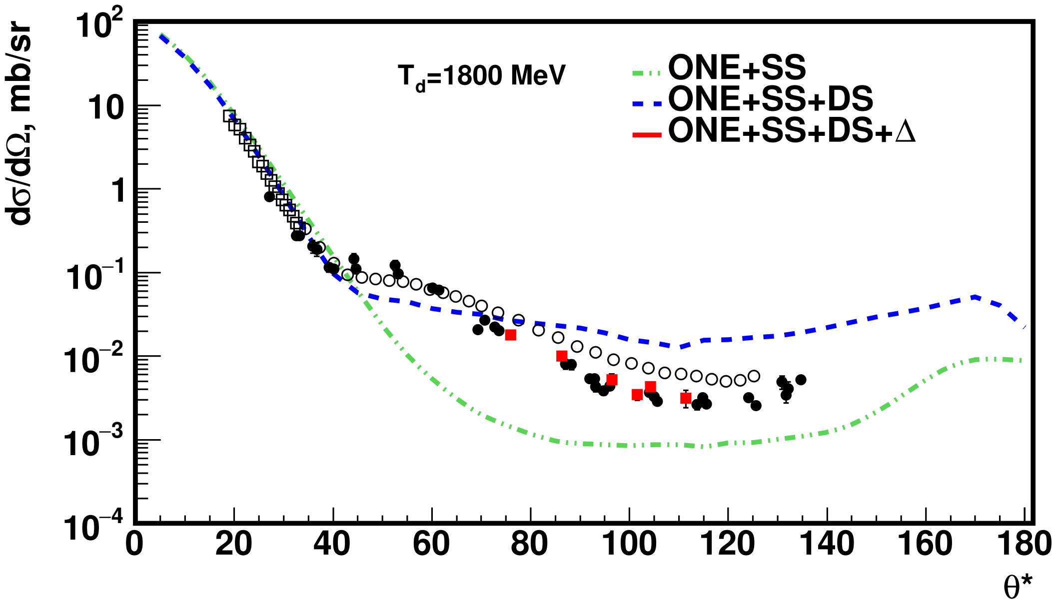

○ - E.Gülmez et al., Phys.Rev.C42, p.2067, 1991, $T_d = 1.585 GeV$

△ - E.Gülmez et al., Phys.Rev.C42, p.2067, 1991, $T_d = 1.286 GeV$

■ - A.A. Terekhin, et al., Eur. Phys. J. A55, 129(2019)

□ - C. Fritzsch et al., Phys.Lett.B 784, 277 (2018), $T_d = 1.8 GeV$

● -Bennet et al., Phys. Rev. Lett. 19, p.387 (1967), $T_d = 2 GeV$

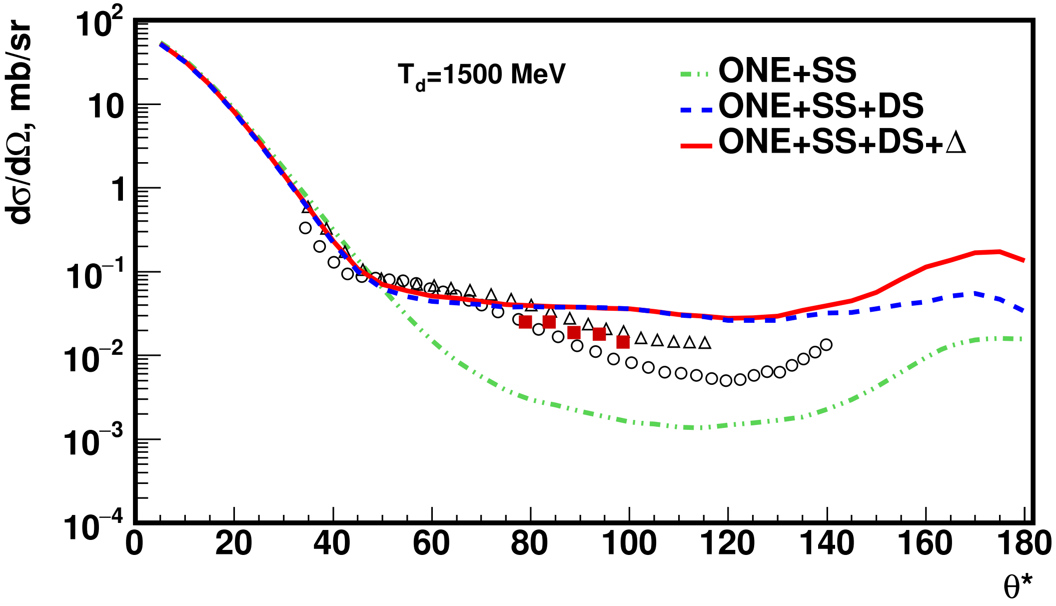

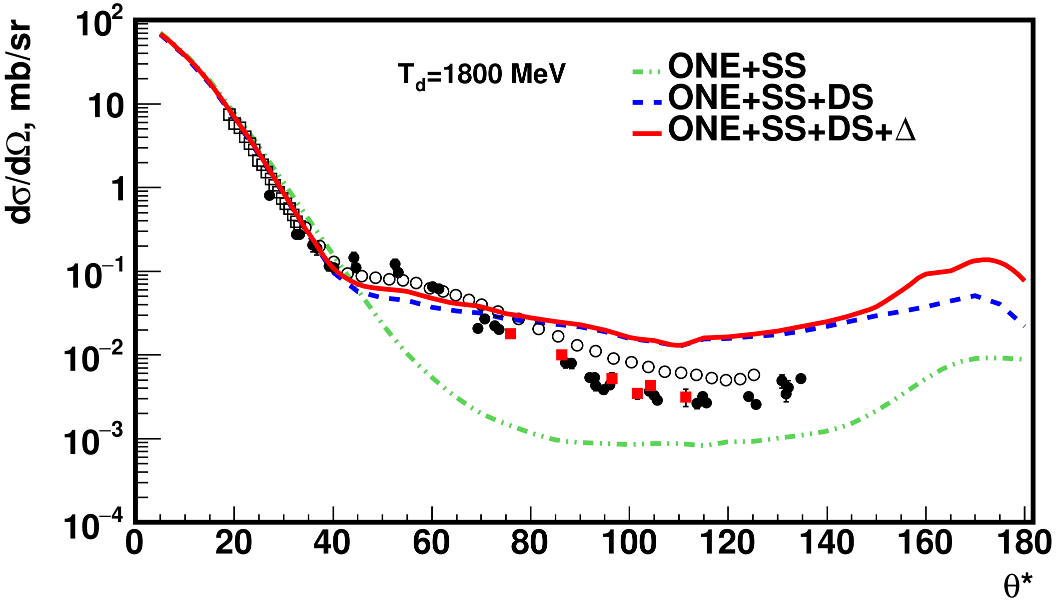

○ - E.Gülmez et al., Phys.Rev.C42, p.2067, 1991, $T_d = 1.585\,GeV$

△ - E.Gülmez et al., Phys.Rev.C42, p.2067, 1991, $T_d = 1.286\,GeV$

■ - A.A. Terekhin, et al., Eur. Phys. J. A55, 129(2019)

□ - C. Fritzsch et al., Phys.Lett.B 784, 277 (2018), $T_d = 1.8\,GeV$

● -Bennet et al., Phys. Rev. Lett. 19, p.387 (1967) , $T_d = 2\,GeV$

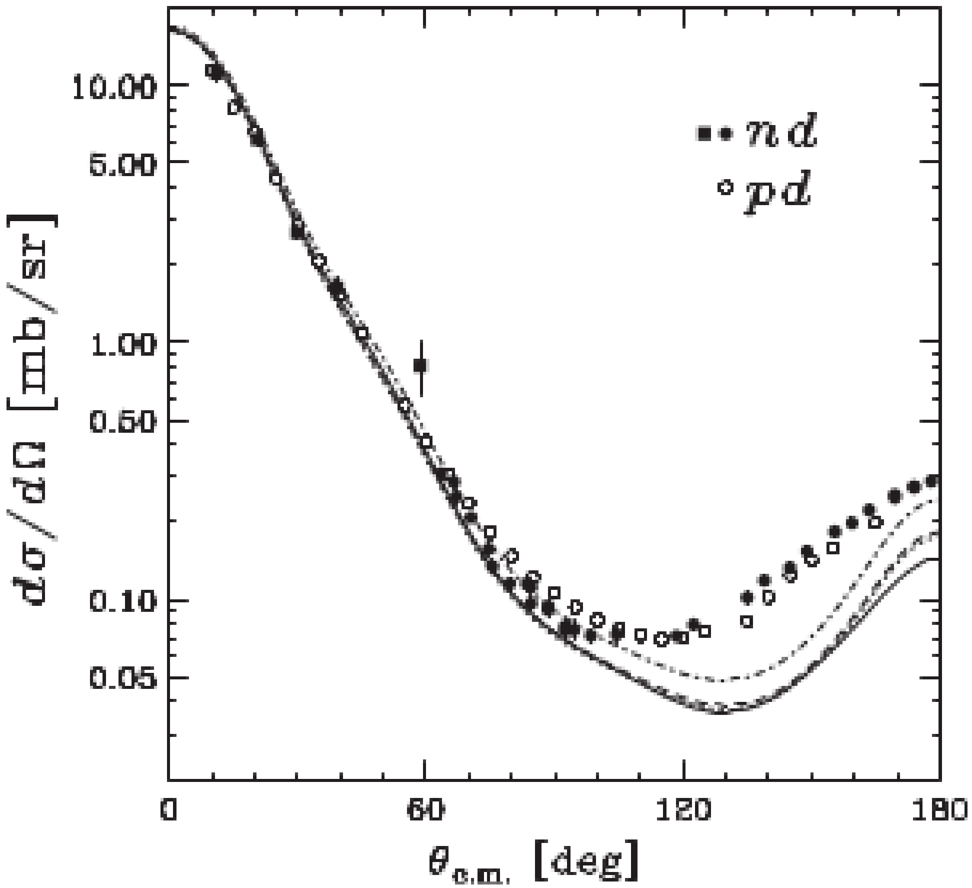

Y.Maeda et al., Phys.Rev.C 76, 014004 (2007), T_N=250 MeV

Solid line is the result of nonrelativistic Faddeev calculation with CD Bonn potential. Relativistic predictions are shown by the dashed, dotted, and dash-dotted lines.

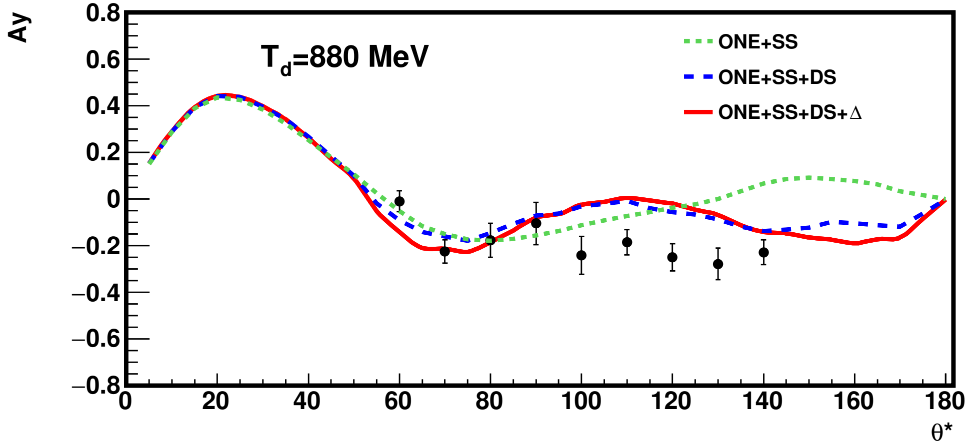

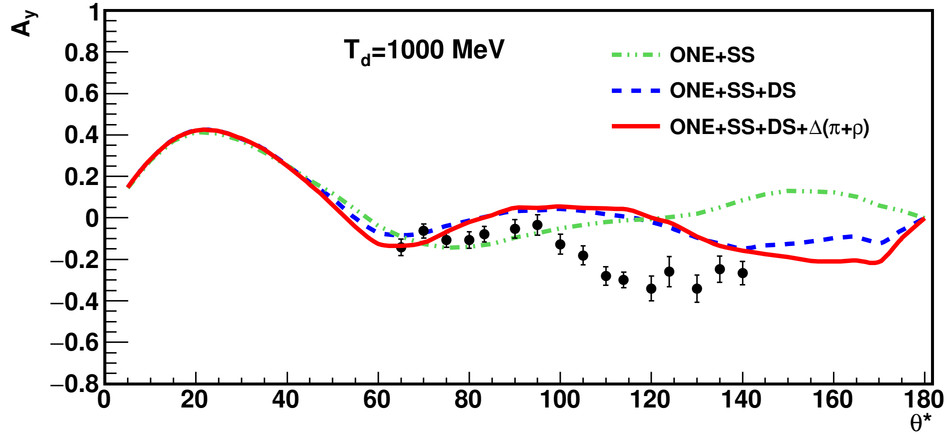

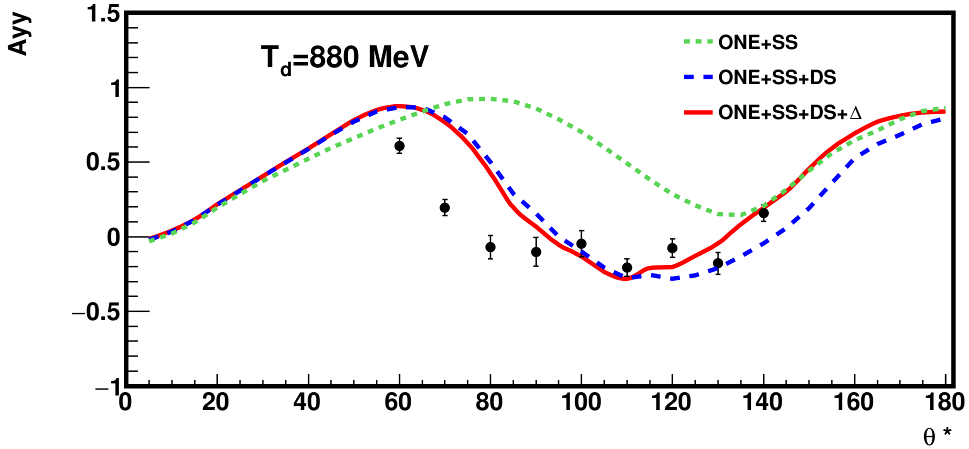

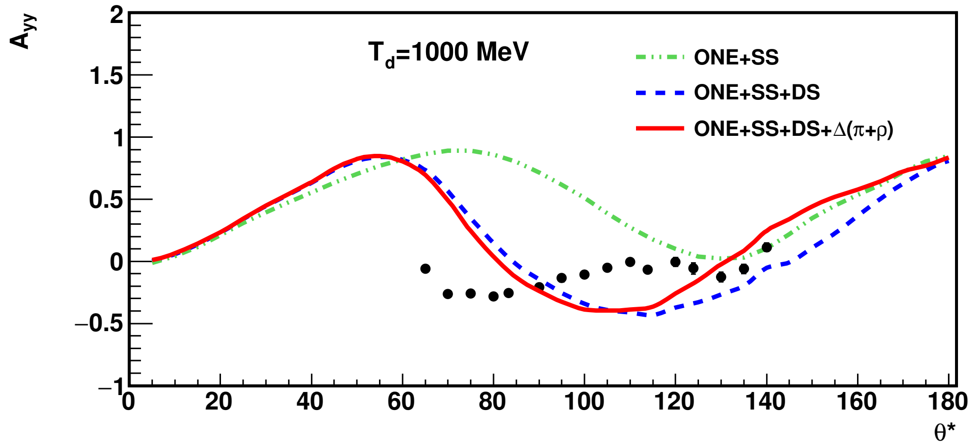

P.K.Kurilkin et al., Phys.Lett.B 715, 61, 2012

M.Janek et al. Physics of Particles and Nuclei, 54,p.595, 2023

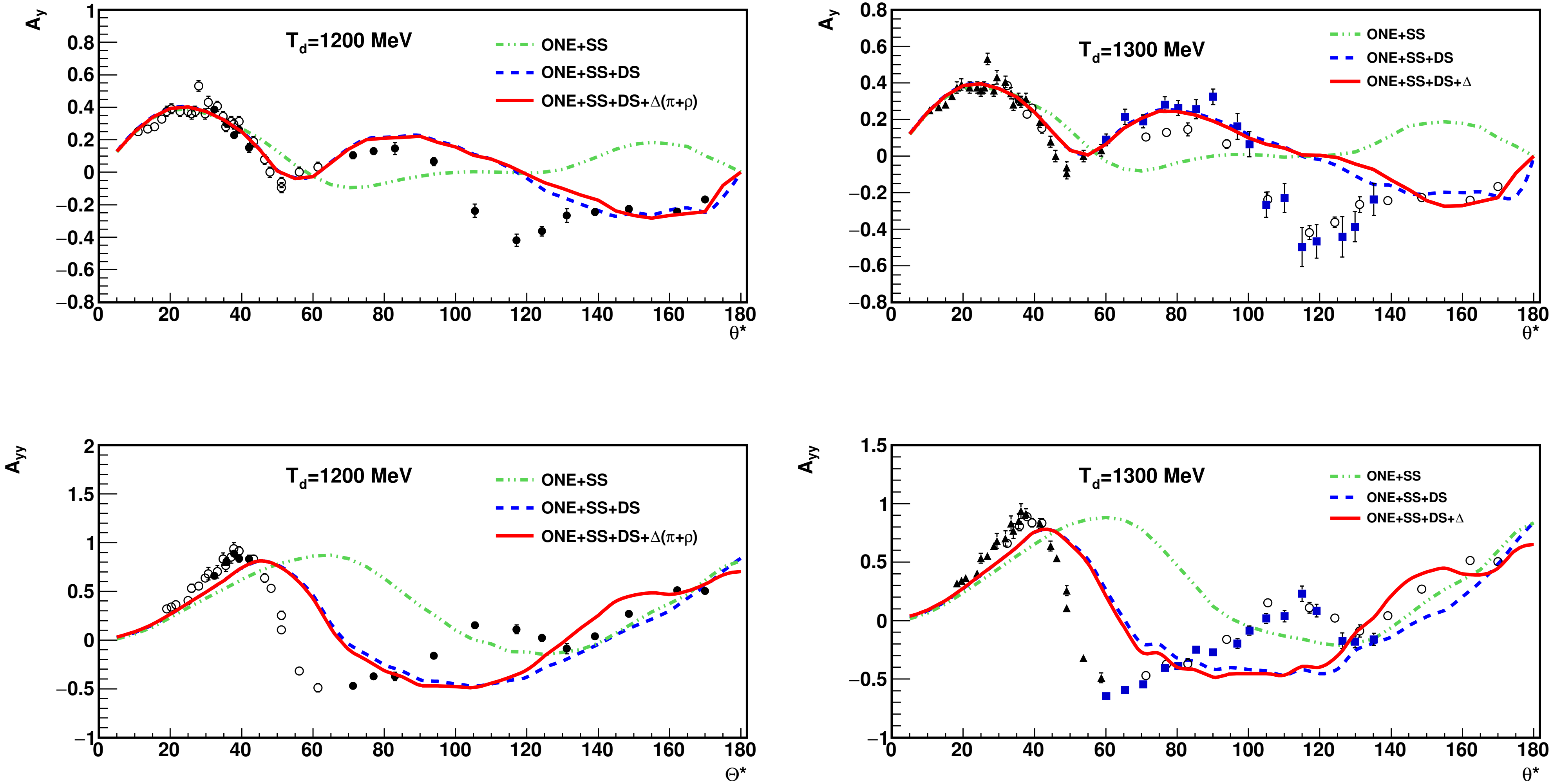

●J.Arvieux et al.,Nucl.Phys.A431, 613 (1984)

○—M.Haji-Saied et al. Phys.Rev. C36, p.2010 (1997)

■ V.P.Ladygin et al.Spin Physics at Nuclotron: Status and Perspectives PoS SPIN2023 (2024) 245

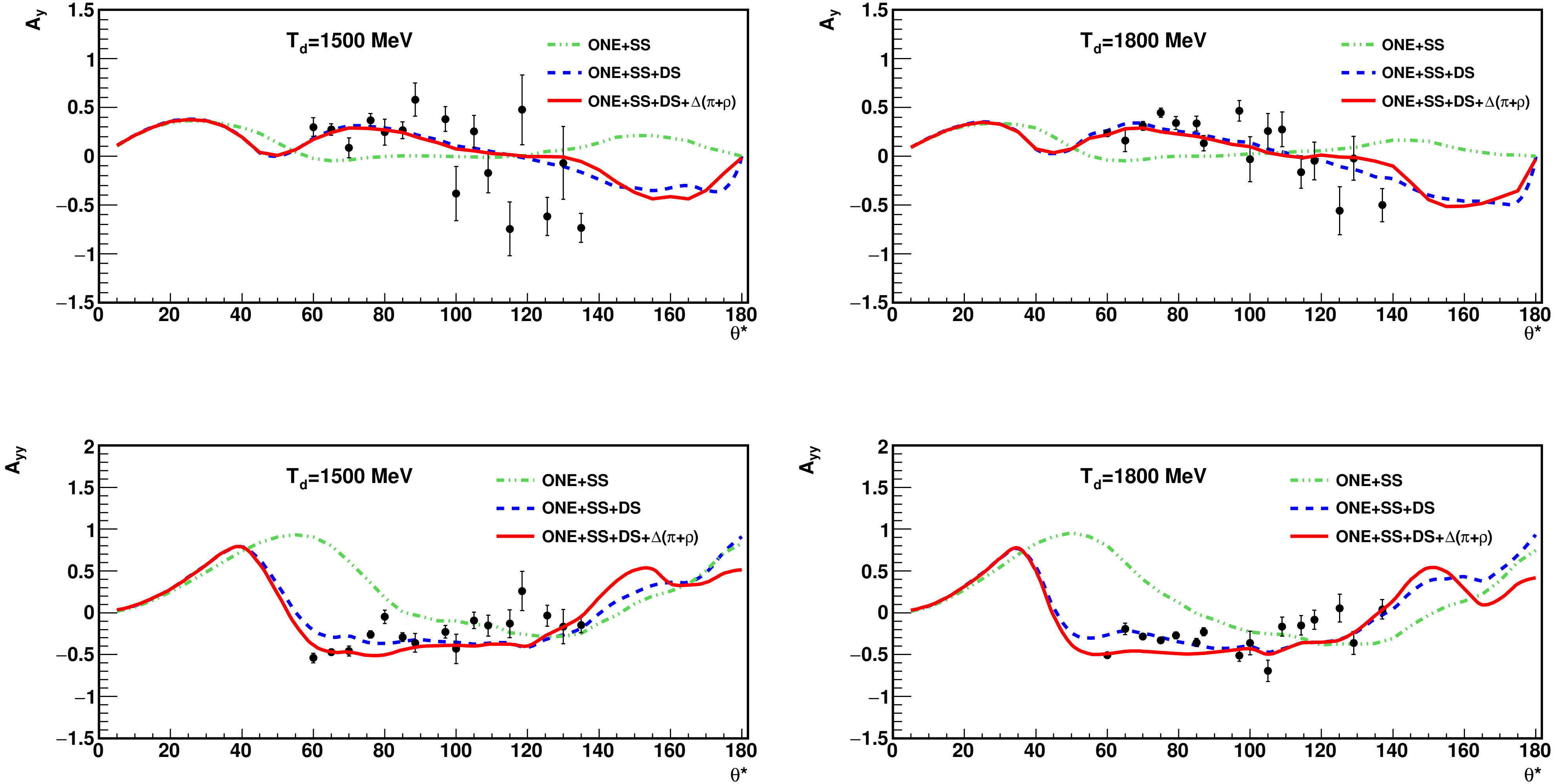

M.Janek et al., Physics of Particles and Nuclei,54, p.595, 2023

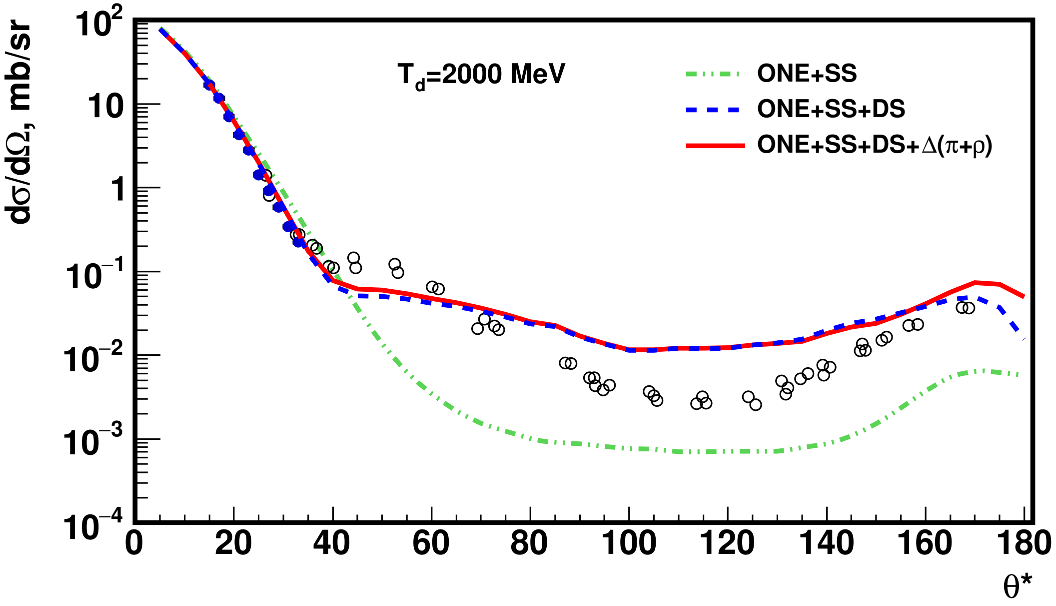

○-Bennet et al., Phys. Rev. Lett. 19, p.387 (1967)

●,●-V.V.Glagolev, V.P.Ladygin, N.B.Ladygina, A.A.Terekhin, Eur.Phys.J. A48, p.182 (2012)

□-M.Haji-Saied et al. Phys.Rev. C36, p.2010 (1997)

■-P.K.Kurilkin et al, Hadron 2011

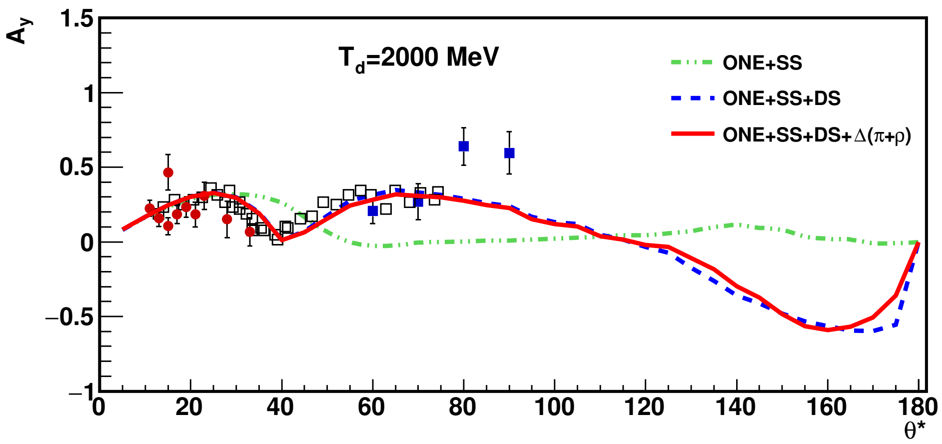

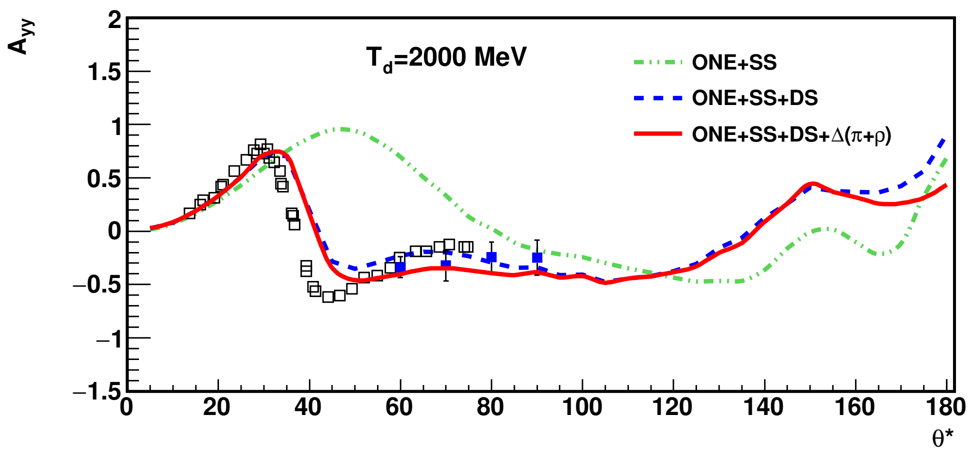

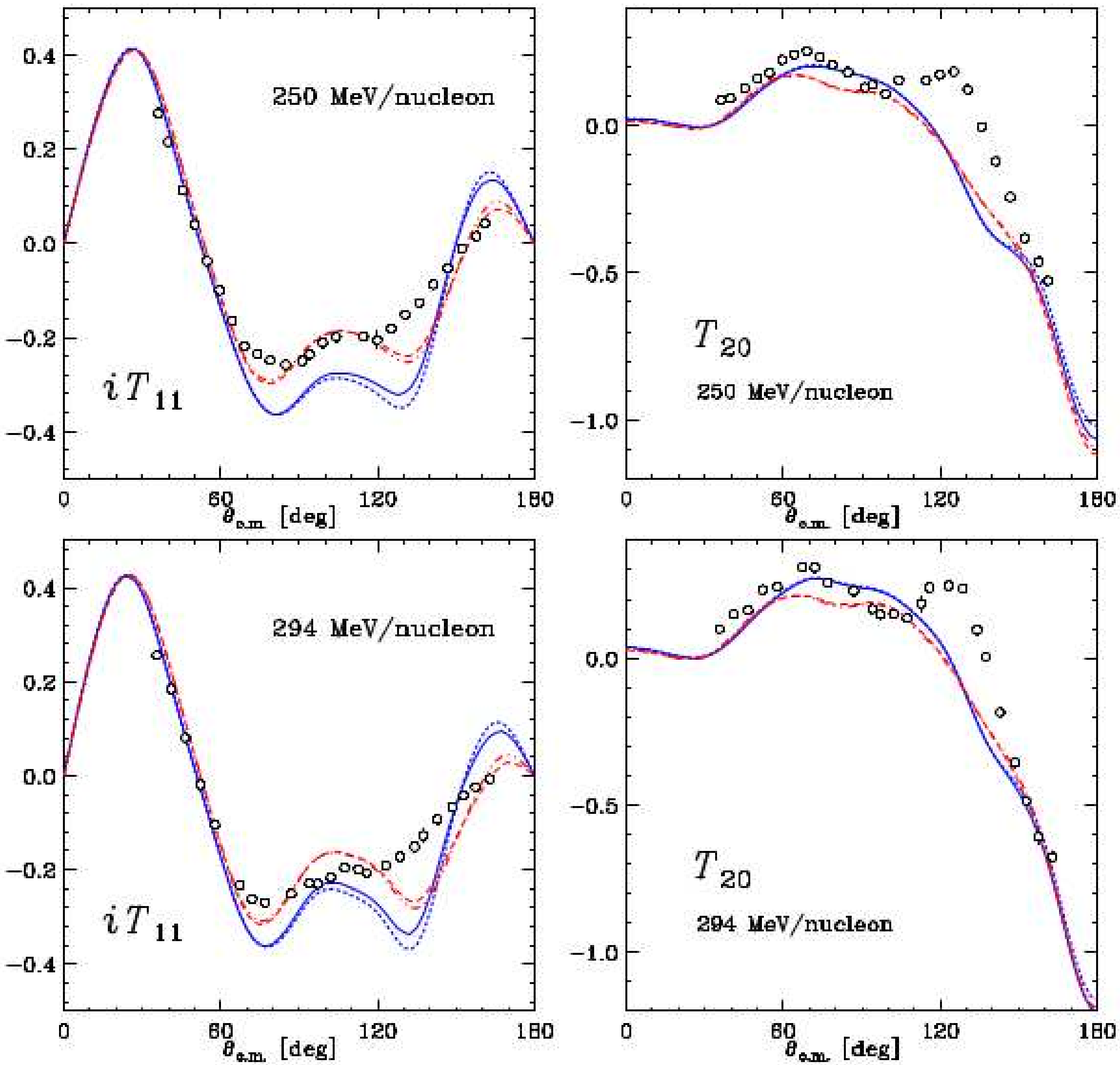

K.Sekiguchi et al.,Phys.Rev. C 89, 064007 (2014)

Deuteron analyzing powers iT11, T20. The solid blue and dashed red curves show the results of non-relativistic Faddeev calculations with the CD Bonn potential alone and combined with the TM99 3NF, respectively. The relativistic calculations based on the CD Bonn potential without Wigner spin rotations are shown with blue dotted curves. The red double-dot-dashed curves show the relativistic calculations with the TM99 3NF included.

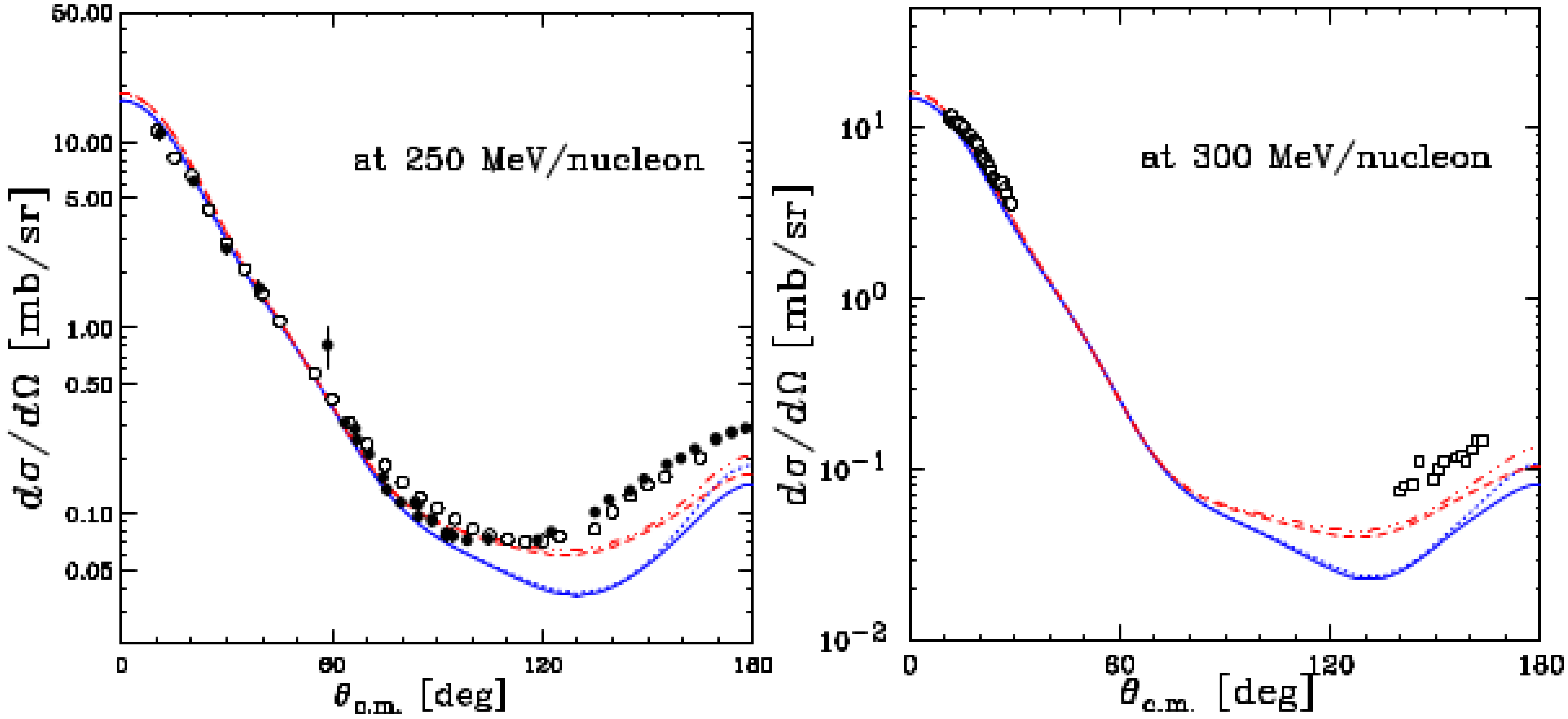

K.Sekiguchi et al.,Phys.Rev. C 89, 064007 (2014)

The solid blue and dashed red curves show the results of nonrelativistic Faddeev calculations with the CD Bonn potential alone and combined with the TM99 3NF, respectively.

Energy dependence of the differential cross section at $\theta^* = 180^0$

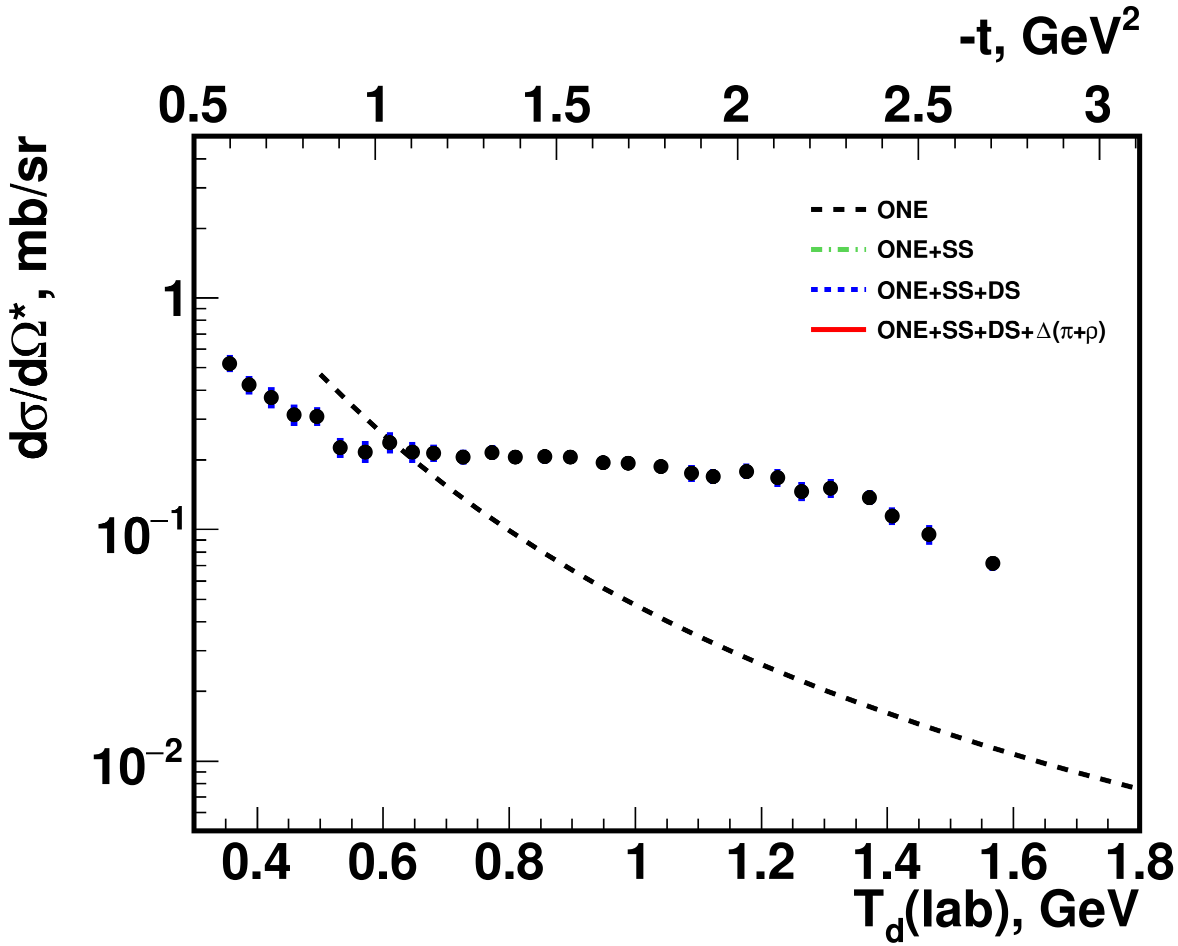

• - B.E.Bonner et al.,Phys.Rev.Lett.39, p.1253 (1977)

Energy dependence of the differential cross section at $\theta^* = 180^0$

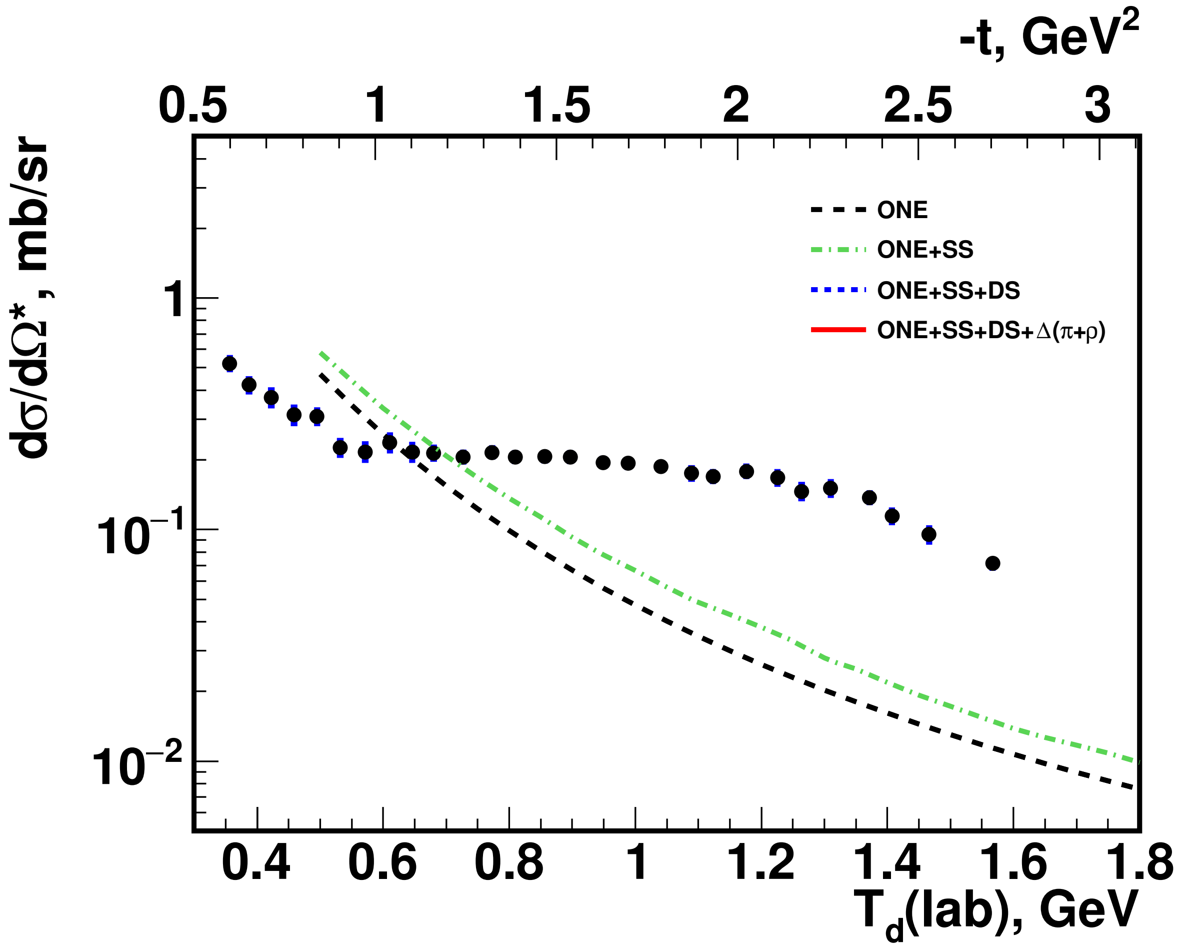

• - B.E.Bonner et al.,Phys.Rev.Lett.39, p.1253 (1977)

Energy dependence of the differential cross section at $\theta^* = 180^0$

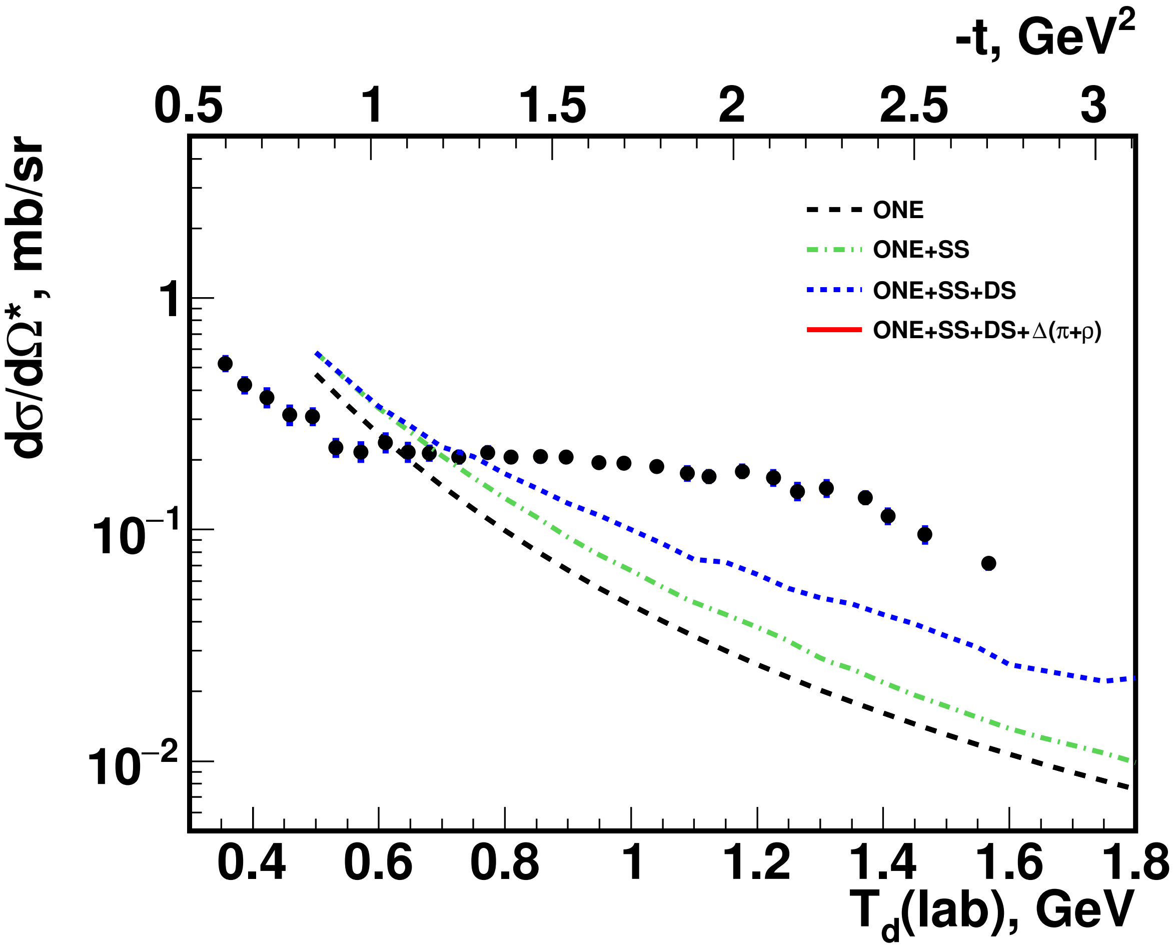

● - B.E.Bonner et al.,Phys.Rev.Lett.39, p.1253 (1977)

Energy dependence of the differential cross section at $\theta^* = 180^0$

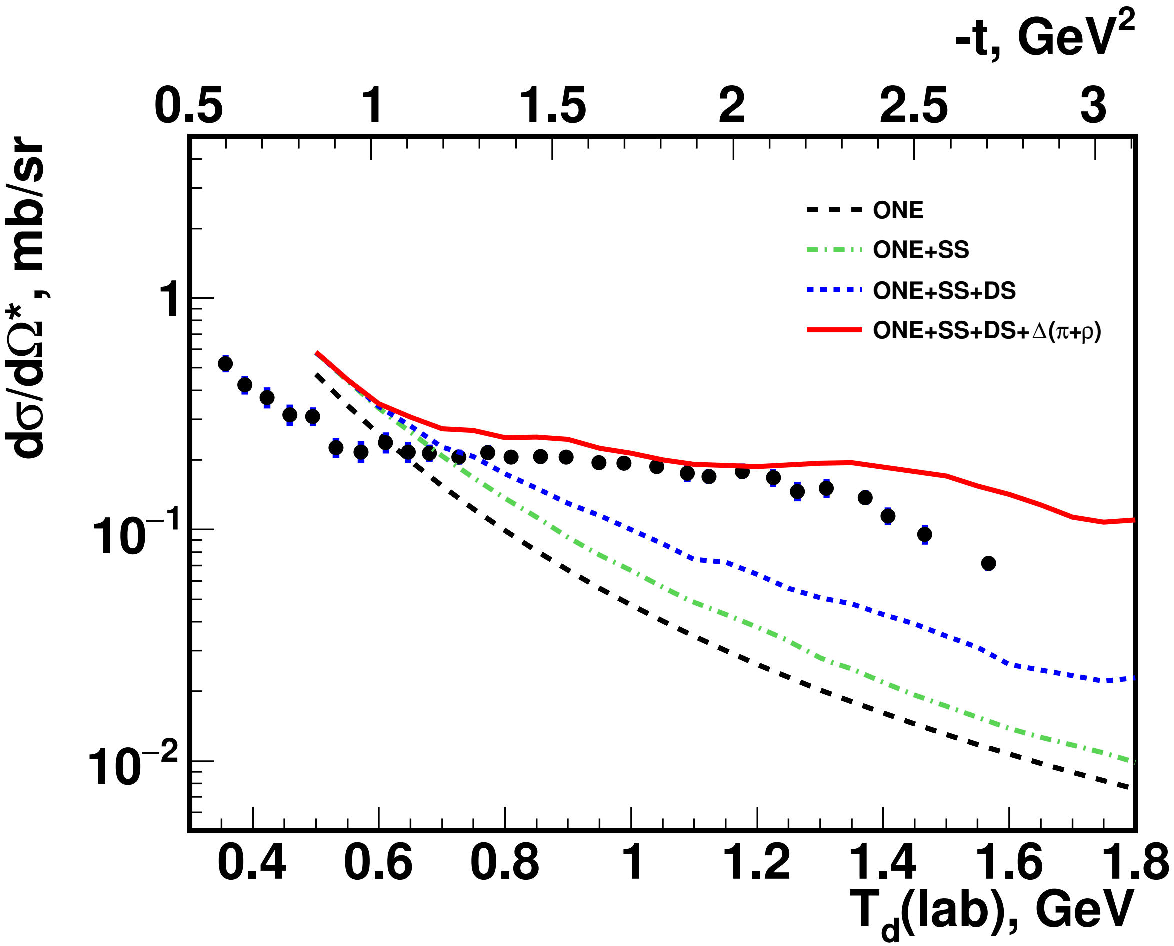

• - B.E.Bonner et al.,Phys.Rev.Lett.39, p.1253 (1977)

Tenzor analyzing power T_{20} at $\theta^* = 180^0$

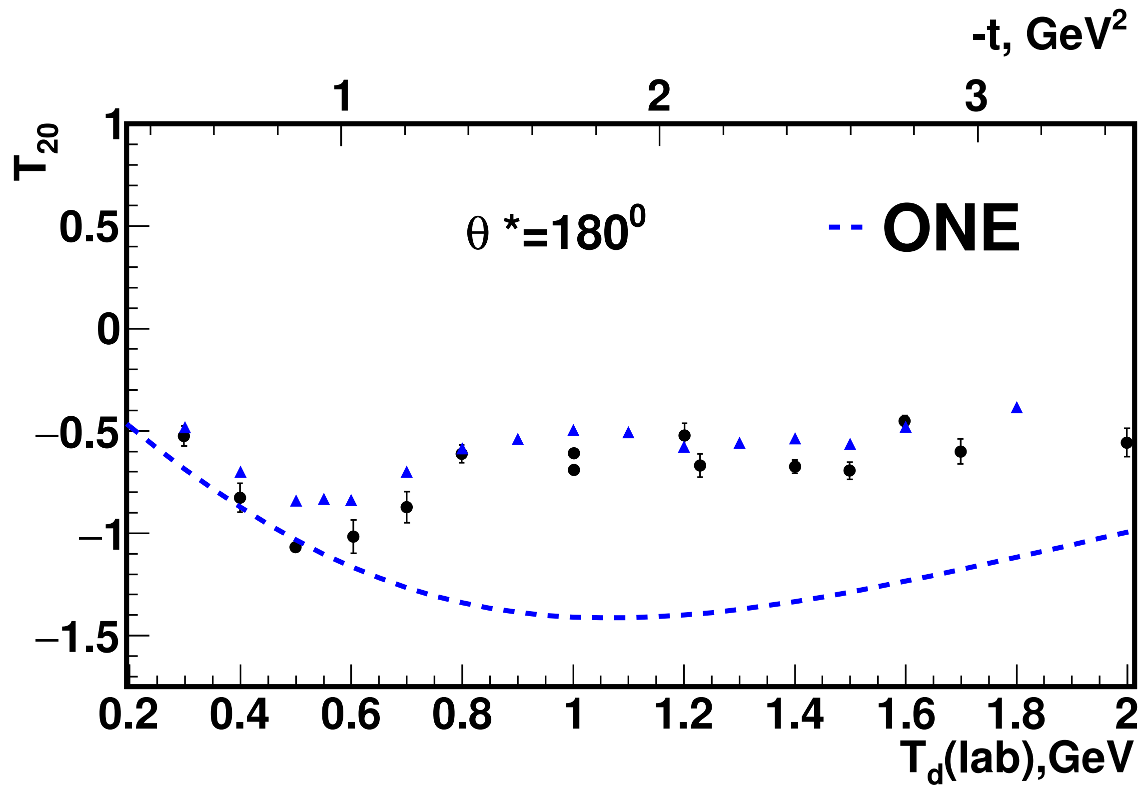

● - J.Arvieux et al.,Nucl.Phys.A431, p.613 (1984)

▲ - V.Punjabi et al.,Phys.Let.B350, p.178 (1995)

Tenzor analyzing power T_{20} at $\theta^* = 180^0$

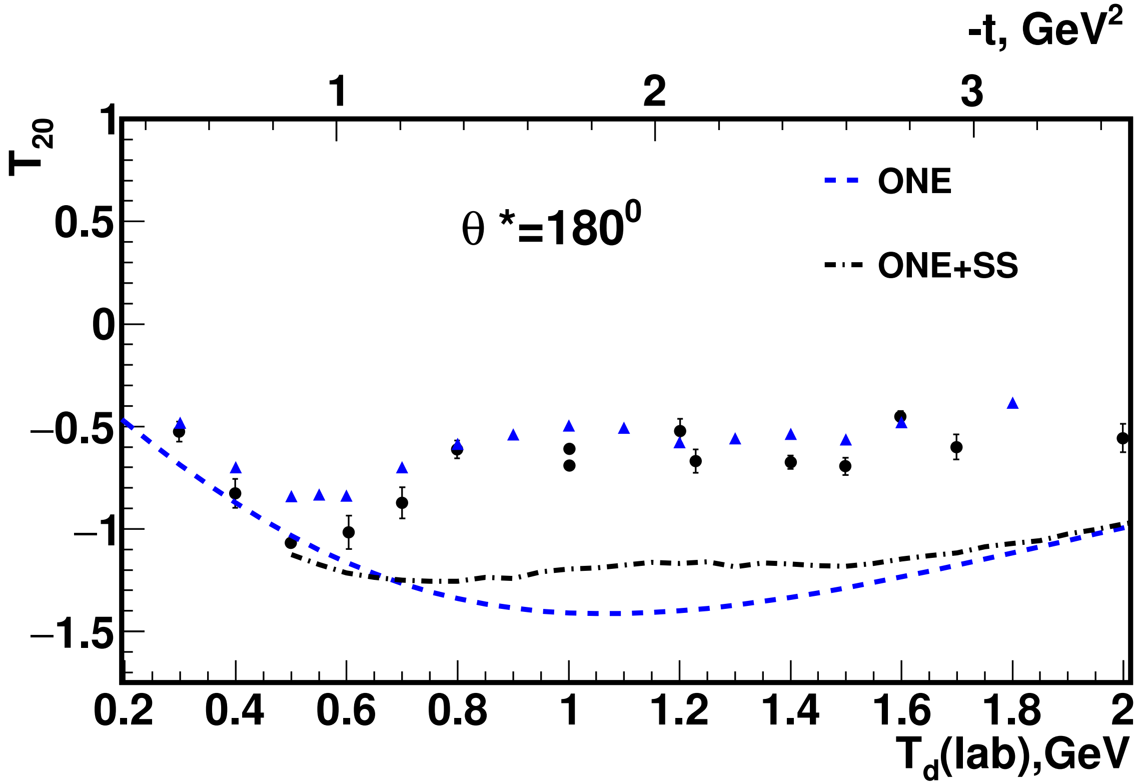

● - J.Arvieux et al.,Nucl.Phys.A431, p.613 (1984)

▲ - V.Punjabi et al.,Phys.Let.B350, p.178 (1995)

Tenzor analyzing power T_{20} at $\theta^* = 180^0$

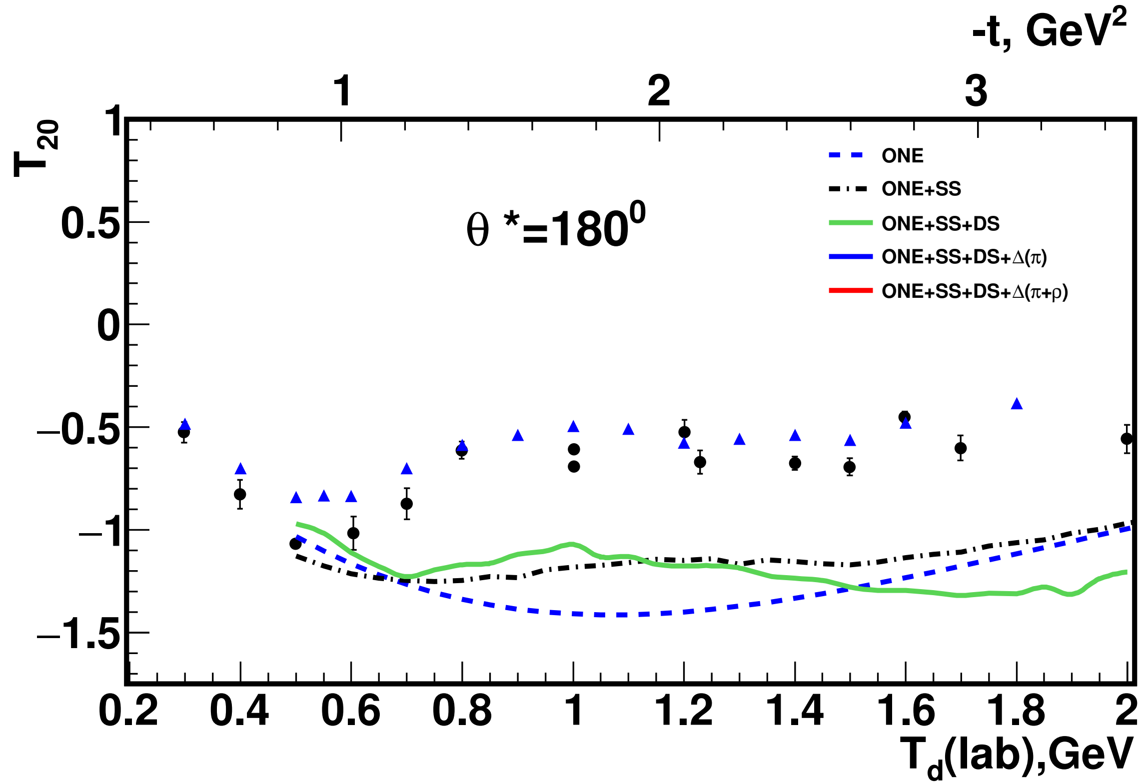

● - J.Arvieux et al.,Nucl.Phys.A431, p.613 (1984)

▲ - V.Punjabi et al.,Phys.Let.B350, p.178 (1995)

Tenzor analyzing power T_{20} at $\theta^* = 180^0$

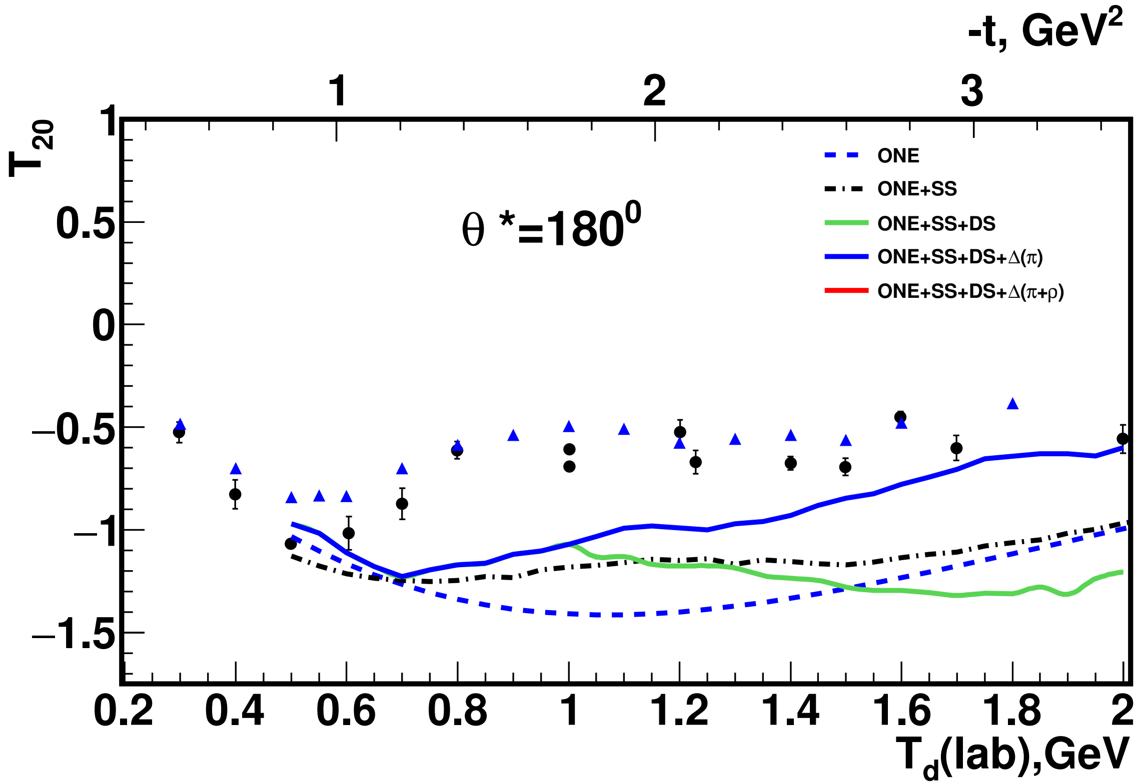

● - J.Arvieux et al.,Nucl.Phys.A431, p.613 (1984)

▲ - V.Punjabi et al.,Phys.Let.B350, p.178 (1995)

Tenzor analyzing power T_{20} at $\theta^* = 180^0$

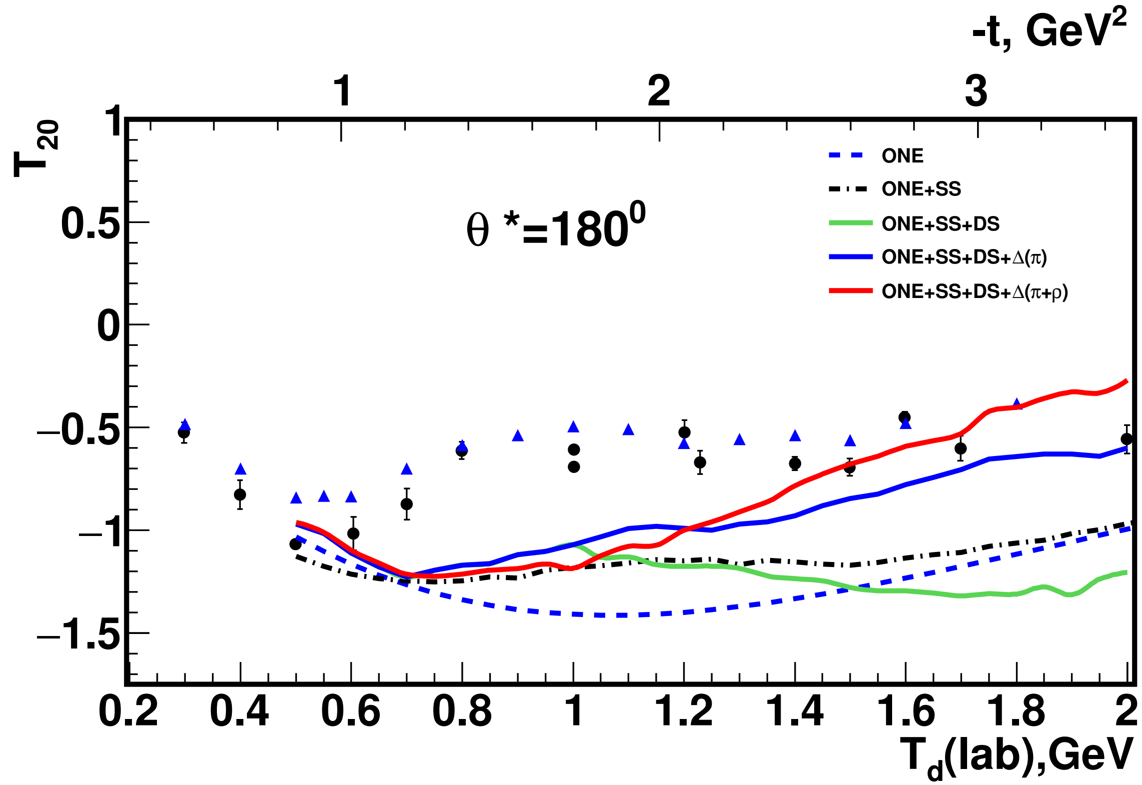

● - J.Arvieux et al.,Nucl.Phys.A431, p.613 (1984)

▲ - V.Punjabi et al.,Phys.Let.B350, p.178 (1995)

Polarisation transfer in $\vec{d}p \to d\vec{p}$ at $\theta^* = 180^0$

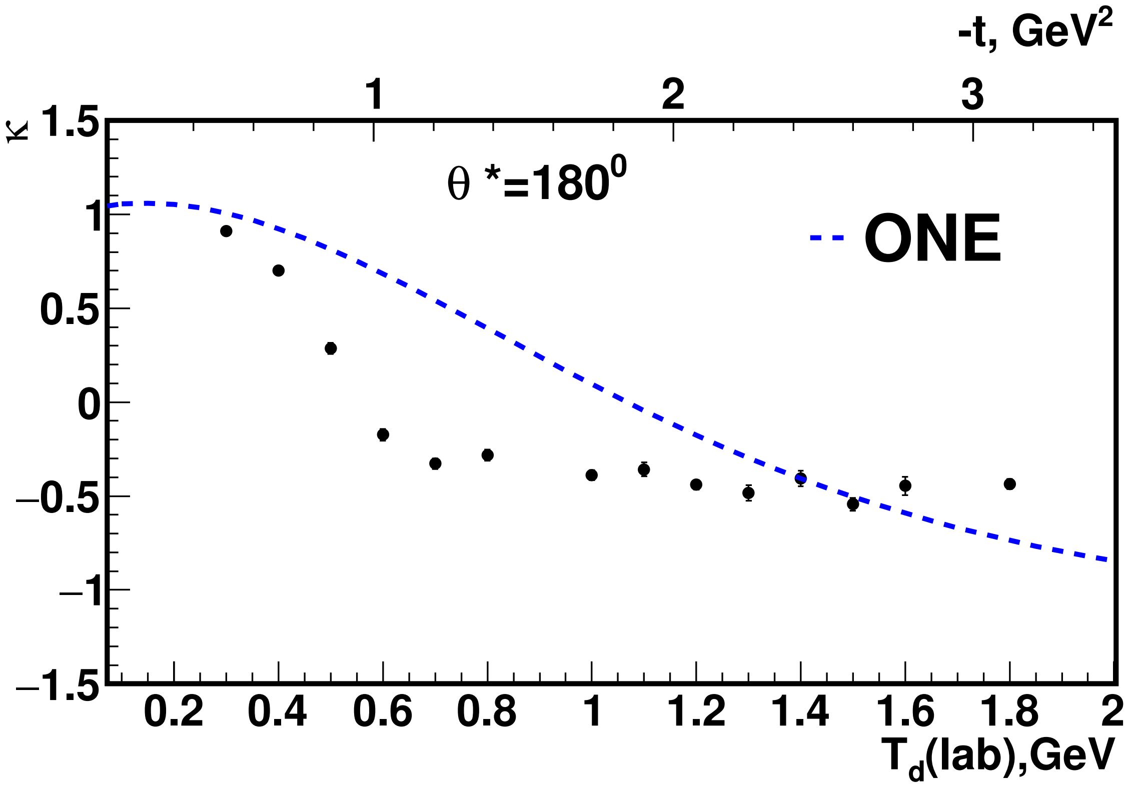

- V.Punjabi et al.,Phys.Let.B350, p.178 (1995)

Polarisation transfer in $\vec{d}p \to d\vec{p}$ at $\theta^* = 180^0$

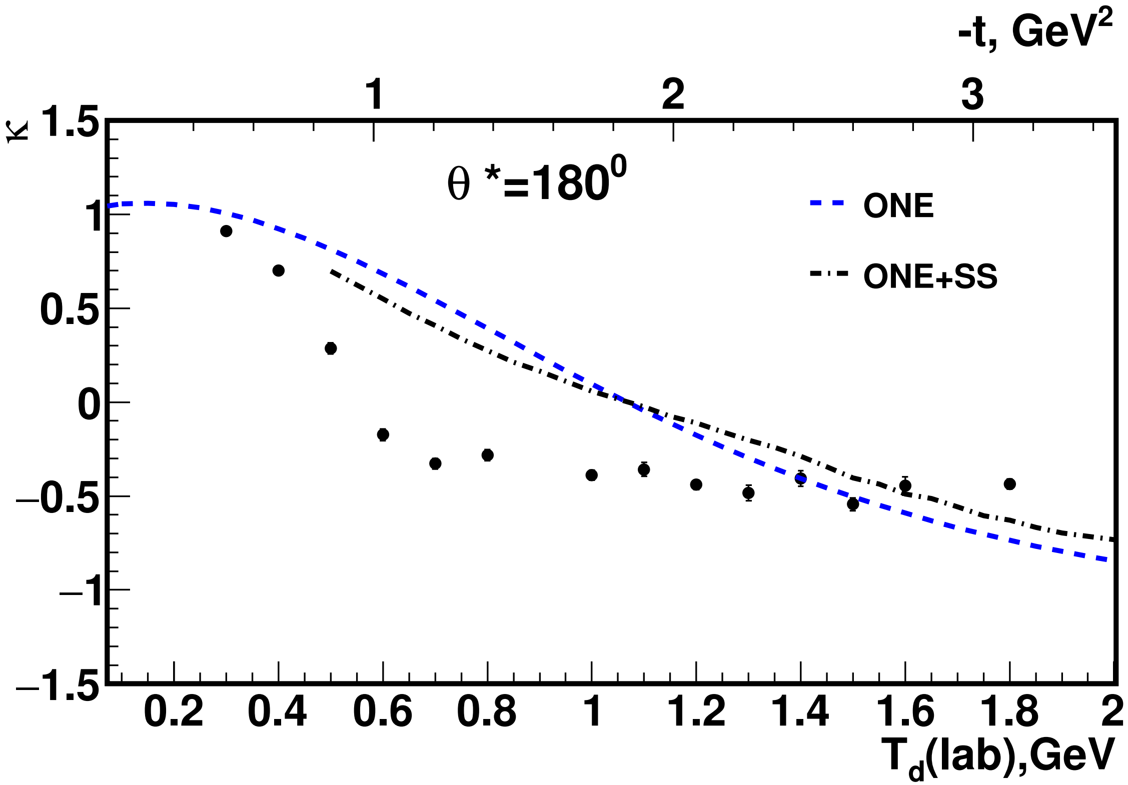

• - V.Punjabi et al.,Phys.Let.B350, p.178 (1995)

Polarisation transfer in $\vec{d}p \to d\vec{p}$ at $\theta^* = 180^0$

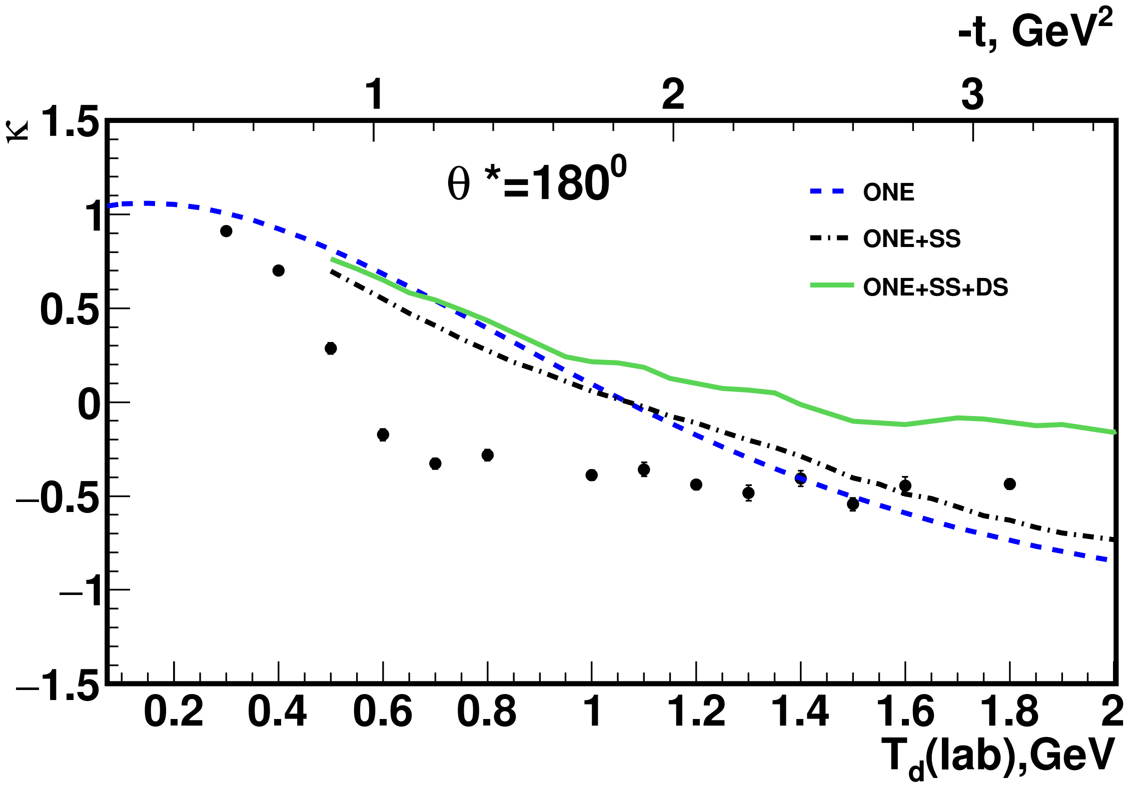

- • - V.Punjabi et al.,Phys.Let.B350, p.178 (1995)

Polarisation transfer in $\vec{d}p \to d\vec{p}$ at $\theta^* = 180^0$

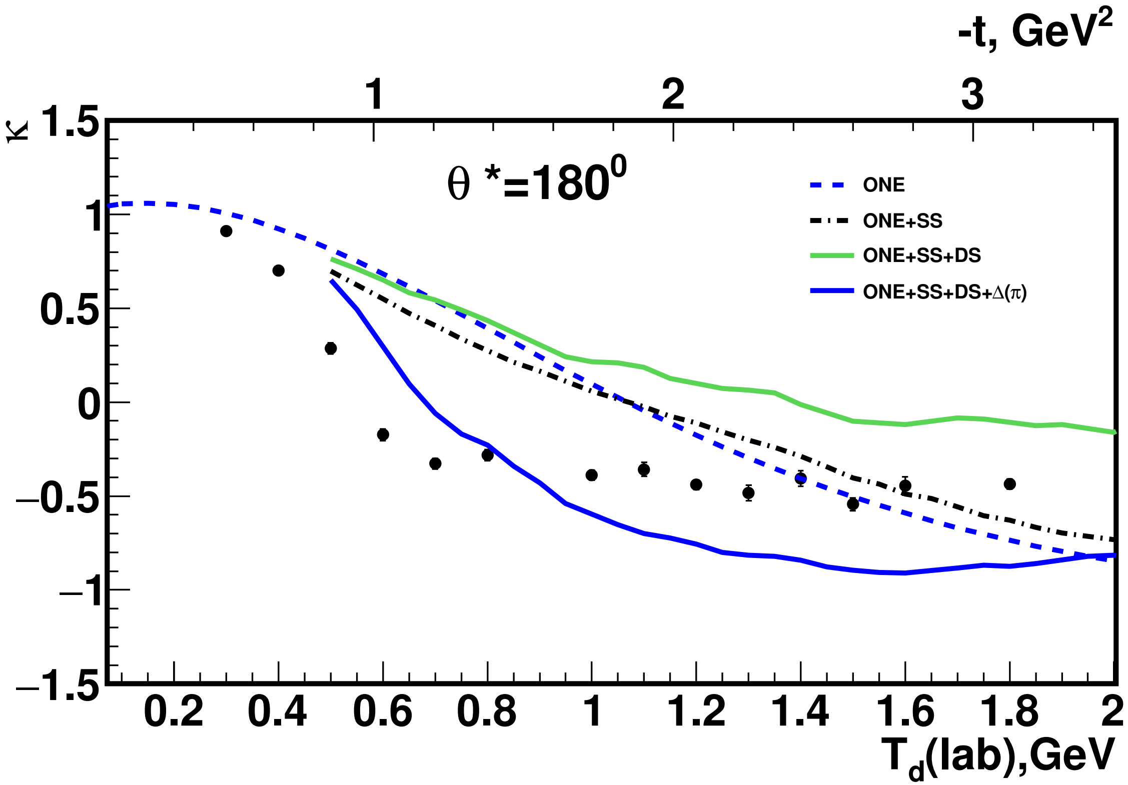

• - V.Punjabi et al.,Phys.Let.B350, p.178 (1995)

Polarisation transfer in $\vec{d}p \to d\vec{p}$ at $\theta^* = 180^0$

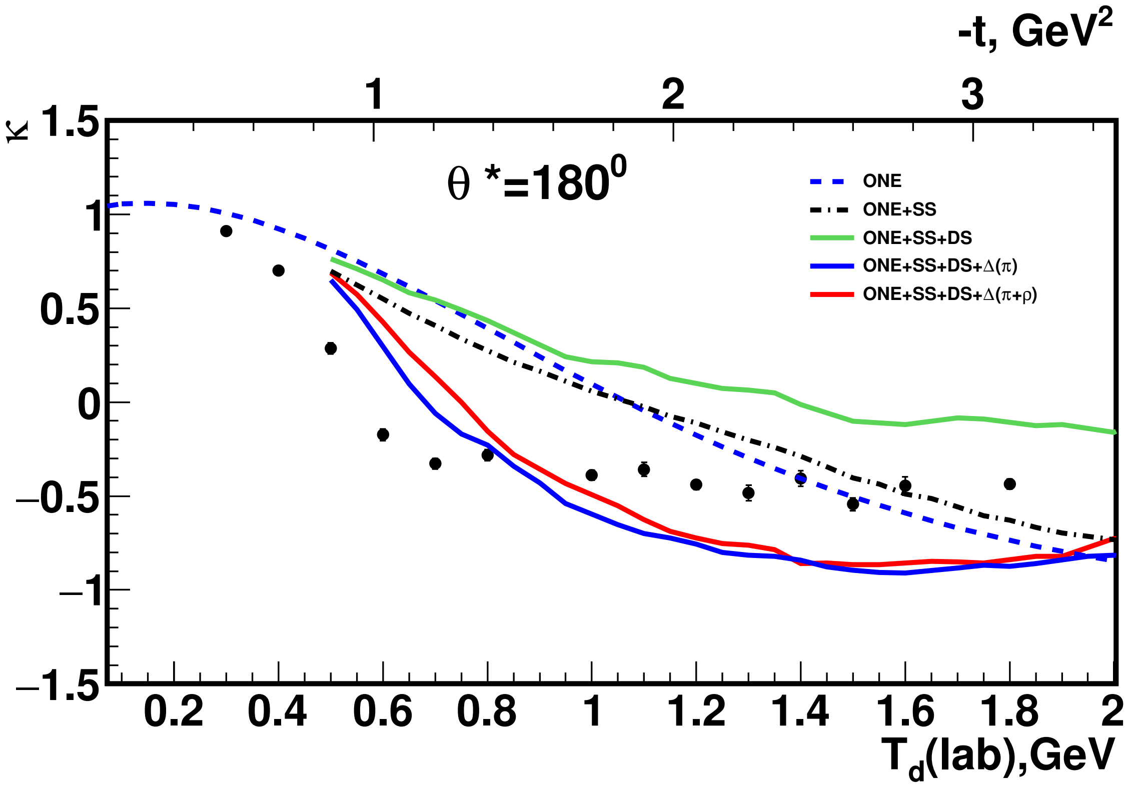

• - V.Punjabi et al.,Phys.Let.B350, p.178 (1995)

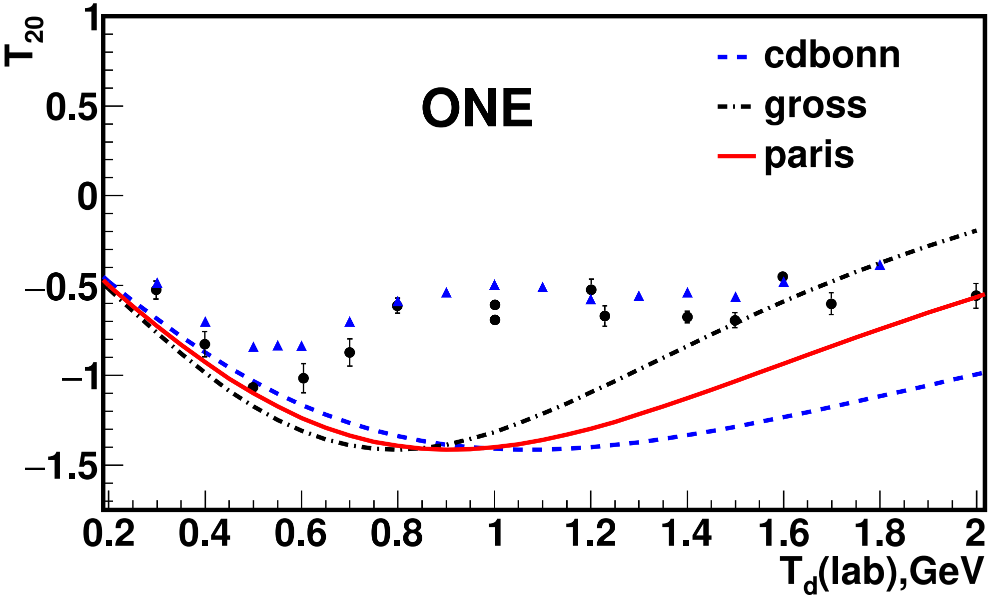
T20
ONE
cdbonn
gross
paris
Td(lab),GeV

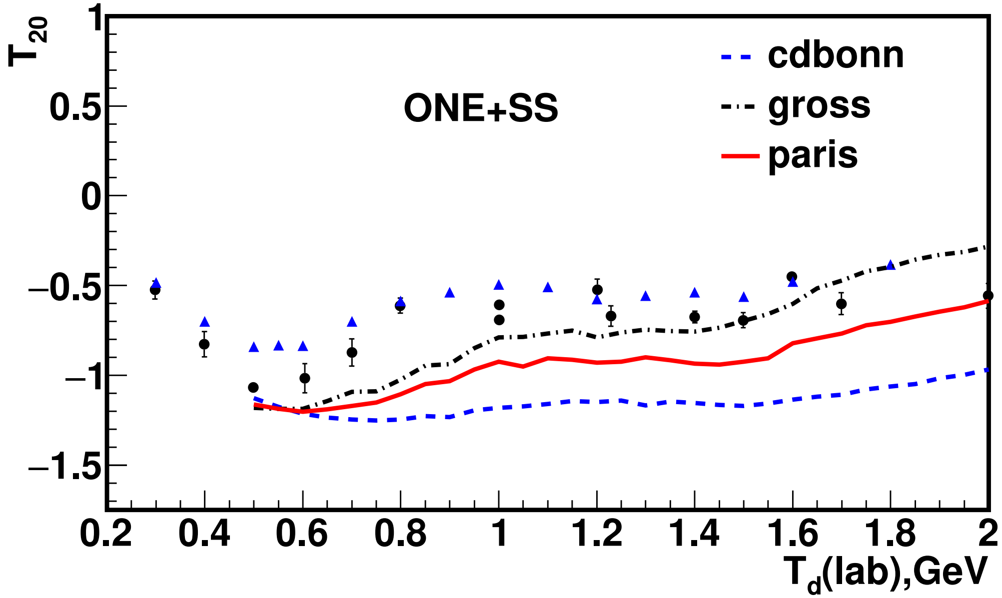
T20
ONE+SS
cdbonn
gross
paris
Td(lab),GeV

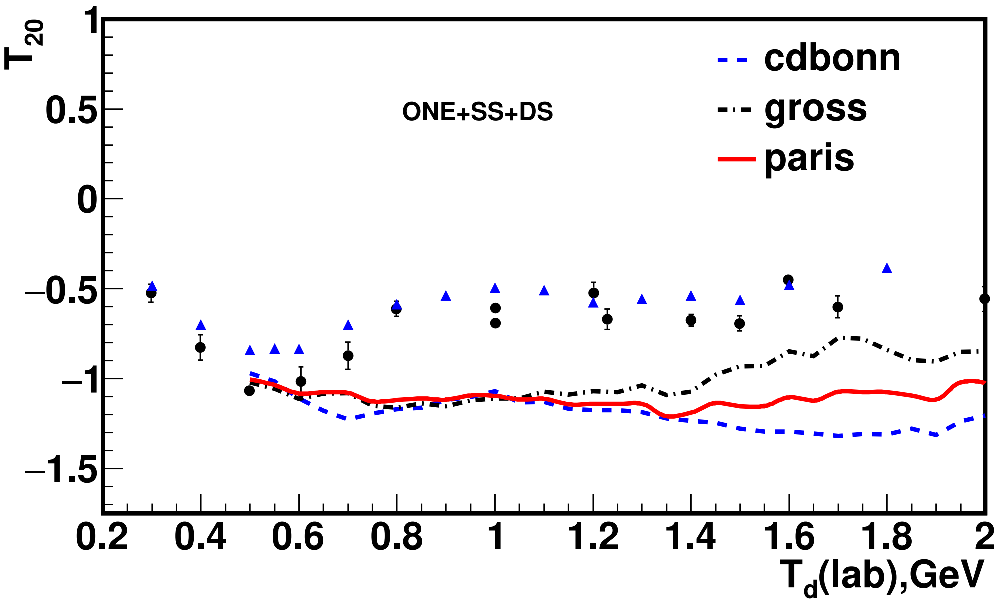
T20
ONE+SS+DS
cdbonn
gross
paris
Td(lab),GeV

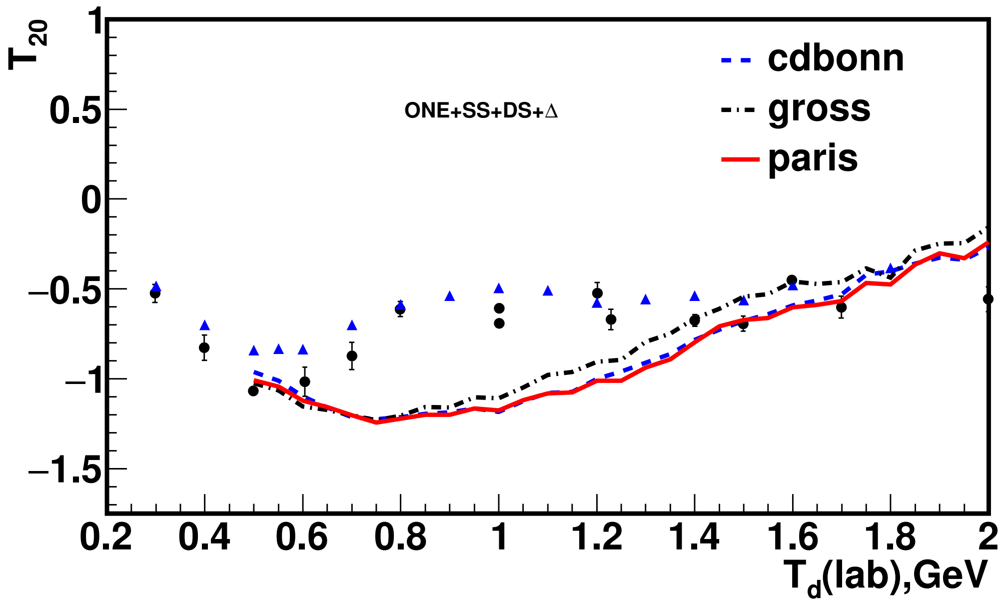
T20
ONE+SS+DS+Δ
cdbonn
gross
paris
Td(lab),GeV

Conclusion

- dp backward elastic scattering has been considered taking into account four contributions: one-nucleon-exchange, single-scattering, double-scattering, and Δ-excitation in an intermediate state.
- **A good description of the differential cross section has been obtained at the scattering angle $\theta^* \leq 90^\circ$ in the energy range between 880 and 2000 MeV.**
- Inclusion of the Δ-isobar term into consideration allows to describe the rise of the differential cross section at $\theta^* \geq 140^\circ$.
- **A quite good description of the data on vector A_y and teszor A_{yy} analyzing powers has been obtained in the whole angular range at the deuteron energies T_d=880, 1500, 1800, 2000 MeV.**
- There are the problems whith the description of the differential cross section at the scattering angles $90^\circ < \theta^* \leq 140^\circ$ in the whole energy range and A_y and A_{yy} at these angles at T_d= 1000, 1200, 1300 MeV.

- **The reaction mechanisms have been also studied at the scattering angle $\theta^* = 180^\circ$. It has been obtained a quite good agreement between the experimental data and the theoretical predictions for the energy dependence of the differential cross section.**
- **Some progress has been achieved in the description of the tensor analyzing power T_{20} and polarisation transfer κ.**

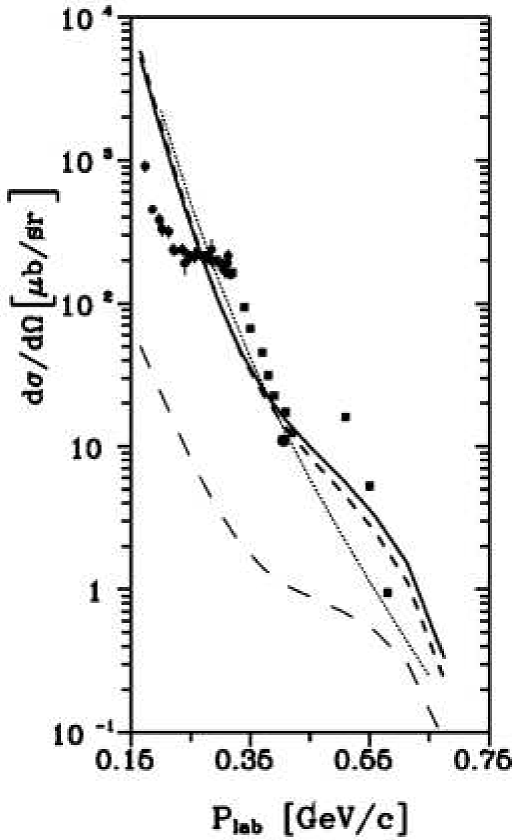

FIG. 2. The spin averaged differential cross section $d\sigma/d\Omega$ for the elastic proton-deuteron backward scattering in the c.m.s. as a function of the momentum of the detected proton in the laboratory system. Dashed line: contribution of the positive-energy BS waves; long-dashed line: contribution of the Lorentz-boost effects Eq. (51); solid line: full BS calculations; dotted line: results of calculations within the nonrelativistic limit with the Bonn potential wave function. Experimental data from [20,36].

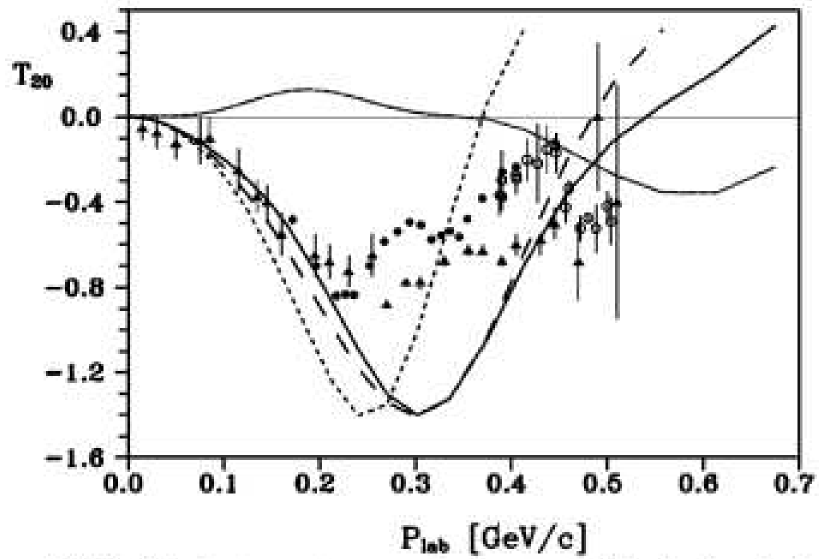

FIG. 3. The deuteron tensor analyzing power T_{20} for the elastic proton-deuteron backward scattering. Long-dashed line: contribution of the positive energy BS waves Eq. (52); dotted line: purely relativistic corrections computed by Eq. (55); solid line: results of computation within the BS approach Eq. (55); short-dashed line: results of computation within the minimal relativization scheme [39] with Paris potential wave function. Experimental data: circles, elastic backward scattering [7,8,14,15]; triangles, T_{20} measured in the deuteron breakup reaction [6].